

Geochemistry, Geophysics, Geosystems®



RESEARCH ARTICLE

10.1029/2021GC009739

Key Points:

- Fingerprinting of tephra found in the marine sediments recovered at Site U1524 during International Ocean Discovery Program (IODP) Expedition 374, in the Ross Sea, Antarctica
- The tephra matches with ca. 1.3 Ma deposits from a Plinian eruption of Chang Peak volcano, Marie Byrd Land, ca. 1,300 km from Site U1524
- Important volcanological data on the eruptive history and chronostratigraphic marker for early Pleistocene records of West Antarctica

Supporting Information:

Supporting Information may be found in the online version of this article.

Correspondence to:

A. Di Roberto,
alessio.diroberto@ingv.it

Citation:








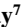

Di Roberto, A., Scateni, B., Di Vincenzo, G., Petrelli, M., Fisauli, G., Barker, S. J., et al. (2021). Tephrochronology and provenance of an early Pleistocene (Calabrian) tephra from IODP Expedition 374 Site U1524, Ross Sea (Antarctica). *Geochemistry, Geophysics, Geosystems*, 22, e2021GC009739. <https://doi.org/10.1029/2021GC009739>

Received 1 MAR 2021
Accepted 9 JUN 2021

Author Contributions:

Conceptualization: A. Di Roberto
Formal analysis: A. Di Roberto, B. Scateni, G. Di Vincenzo, M. Petrelli, G. Fisauli, S. J. Barker, P. Del Carlo, F. Colleoni, D. K. Kulhanek, R. McKay, L. De Santis
Investigation: A. Di Roberto, B. Scateni, G. Di Vincenzo, M. Petrelli, G. Fisauli, S. J. Barker

Tephrochronology and Provenance of an Early Pleistocene (Calabrian) Tephra From IODP Expedition 374 Site U1524, Ross Sea (Antarctica)

A. Di Roberto¹ , B. Scateni¹, G. Di Vincenzo² , M. Petrelli³ , G. Fisauli³, S. J. Barker⁴ , P. Del Carlo¹ , F. Colleoni⁵ , D. K. Kulhanek⁶ , R. McKay⁷ , L. De Santis⁵ , and The IODP Expedition 374 Scientific Party

¹Istituto Nazionale di Geofisica e Vulcanologia (INGV), Sezione di Pisa, Pisa, Italy, ²Istituto di Geoscienze e Georisorse - Consiglio Nazionale delle Ricerche (IGG-CNR), Pisa, Italy, ³Dipartimento di Fisica e Geologia, Università di Perugia, Perugia, Italy, ⁴School of Geography, Environment and Earth Sciences, Victoria University of Wellington, Wellington, New Zealand, ⁵National Institute of Oceanography and Applied Geophysics (OGS), Borgo Grotta Gigante, Trieste, Italy, ⁶International Ocean Discovery Program, Texas A&M University, College Station, TX, USA, ⁷Antarctic Research Centre, Victoria University of Wellington, Wellington, New Zealand

Abstract We present a full characterization of a 20 cm-thick tephra layer found intercalated in the marine sediments recovered at Site U1524 during International Ocean Discovery Program (IODP) Expedition 374, in the Ross Sea, Antarctica. Tephra bedforms, mineral paragenesis, and major- and trace-element composition on individual glass shards were investigated and the tephra age was constrained by ⁴⁰Ar-³⁹Ar on sanidine crystals. The ⁴⁰Ar-³⁹Ar data indicate that sanidine grains are variably contaminated by excess Ar, with the best age estimate of 1.282 ± 0.012 Ma, based on both single-grain total fusion analyses and step-heating experiments on multi-grain aliquots. The tephra is characterized by a very homogeneous rhyolitic composition and a peculiar mineral assemblage, dominated by sanidine, quartz, and minor aenigmatite and arfvedsonite-riebeckite amphiboles. The tephra from Site U1524 compositionally matches with a ca. 1.3 Ma, rhyolitic pumice fall deposit on the rim of the Chang Peak volcano summit caldera, in the Marie Byrd Land, located ca. 1,300 km from Site U1524. This contribution offers important volcanological data on the eruptive history of Chang Peak volcano and adds a new tephrochronologic marker for the dating, correlation, and synchronization of marine and continental early Pleistocene records of West Antarctica.

Plain Language Summary We report important information on the history and character of eruptions of Antarctic volcanoes. The study examines products from past explosive volcanic eruptions (tephra) preserved in marine sediments in the Southern Ocean that surrounds Antarctica. Tephra are invaluable markers for dating and correlating geological units, and can be used for the synchronization of climate proxy records. We present the full characterization of a 20 cm-thick tephra recovered in deep-sea marine sediments at Site U1524 during the International Ocean Discovery Program (IODP) Expedition 374, in the Ross Sea, Antarctica. The morphology of volcanic particles, their mineralogy, and chemical composition of volcanic glasses were assessed and the tephra age was constrained by the ⁴⁰Ar-³⁹Ar method. Results allow to correlate the studied tephra with the deposits of a large explosive (Plinian) eruption from Chang Peak volcano, in the Marie Byrd Land, located c. 1,300 km from the Site U1524. The study of the marine tephra provides glimpses of the history of explosive volcanism from the Marie Byrd Land and constitutes a new, very important chronostratigraphic marker for early Pleistocene records of West Antarctica.

1. Introduction

Knowledge of Antarctic volcanism is extensive but still limited by the scarce exposure of volcanic rocks due to glacial cover. In particular, the record of tephra produced by explosive activity is scarce due to the low possibility of preservation of this type of deposits in highly dynamic polar environments. In the Antarctic continental setting, most of the information on explosive volcanism derive from tephra layers contained in the blue ice records (Curzio et al., 2008; Dunbar et al., 2003; Harpel et al., 2008; Keys et al., 2017; Wilch et al., 1999) and the deep ice-cores records (Narcisi et al., 2012, 2017) both offering important data but mostly limited to the Holocene to late Pleistocene (see Epica Dome ice core record spanning the last 800 ka; Masson-Delmotte et al., 2010). Additionally, marine sediments of the Southern Ocean are a critical resource to draw information on the eruptive

© 2021. The Authors.

This is an open access article under the terms of the [Creative Commons Attribution License](https://creativecommons.org/licenses/by/4.0/), which permits use, distribution and reproduction in any medium, provided the original work is properly cited.

Writing – original draft: A. Di Roberto, B. Scatani, G. Di Vincenzo, M. Petrelli, G. Fisauli, S. J. Barker, P. Del Carlo, R. McKay, L. De Santis

Writing – review & editing: A. Di Roberto, B. Scatani, G. Di Vincenzo, M. Petrelli, G. Fisauli, S. J. Barker, P. Del Carlo, F. Colleoni, D. K. Kulhanek, R. McKay, L. De Santis

history and evolution of volcanism of Antarctica which are complementary to those drawn from on-land studies (Del Carlo et al., 2015; Di Roberto et al., 2019; 2020; 2021; Hillenbrand et al., 2008; Moreton & Smellie, 1998; Oppedal et al., 2018; Smellie, 1999). For example, extensive records of Pleistocene to Miocene volcanoclastic deposits and tephra layers are contained in sequences recovered during international drilling programs (Di Roberto et al., 2021). Such tephra deposits represent a potentially invaluable chronological tool that is essential to date sedimentary archives (Abbott et al., 2018; Di Roberto et al., 2019; Mezgec et al., 2017; Tesi et al., 2020), enable correlation over significant distances, and link and synchronize different paleoclimatic and palaeoenvironmental archives (Davies, 2015; Lane et al., 2017; Lowe, 2011).

Here we report the discovery of a ~20 cm thick tephra layer intercalated in the sediments recovered at Site U1524 during the International Ocean Discovery Program (IODP) Expedition 374, in the Ross Sea, Antarctica. We have characterized the tephra for its texture, mineralogy, major- and trace-element composition obtained on individual glass shards. We dated the tephra by using paleomagnetic age constraints and ^{40}Ar - ^{39}Ar data obtained on sanidine crystals extracted from this horizon. Based on geochemical composition and age, the tephra is correlated with a comenditic Plinian fall deposit cropping out on the rim of the 10-km-wide caldera of Chang Peak volcano, in the Marie Byrd Land, ca. 1,300 km from the coring site. This study presents one of the few Antarctic cases (see for example Di Roberto et al., 2019, 2020; Hillenbrand et al., 2008) in which a marine tephra layer is correlated with reasonable certainty to its source volcano, offering important volcanological data on the eruptive history and intensity of the eruption that generated it. The far-traveled nature and thickness of this tephra imply that it was produced by a large magnitude eruption, probably of Plinian intensity, representing one of the largest eruptions presently recorded in the Marie Byrd Land. We suggest that this tephra could be an important chronological marker in multiple depositional environments that will be a useful target for future deep ice drilling projects and could offer an exceptional possibility of dating and of synchronizing ice sequences with the marine environment.

2. Background - IODP Expedition 374

In 2018, International Ocean Discovery Program (IODP) Expedition 374 (Ross Sea West Antarctic Ice Sheet History) drilled a total of five sites as part of a continental shelf to rise transect designed to understand how past ice sheets and oceanic circulation interact since the Early Miocene. Of these sites, Sites U1524 and U1525 obtained near-continuous high-resolution Plio-Pleistocene sedimentary records preserved on a continental rise levee system near the flank of the Hillary Canyon. However, the upper ~50 m at Site U1525 consists of mass transport deposits emplaced over the past ~0.8 Ma as part of a large trough-mouth fan deposited to the west of the site (McKay et al., 2019c). The lower 100 m at Site U1525 and the entire 400 m of sediment at Site U1524 recovered near-continuous records of the downslope flow of Ross Sea Bottom Water and turbidity currents, alongside records of enhanced iceberg discharge over the site. The expanded sections at Sites U1524 and U1525 consist of finely laminated biogenic and terrigenous material delivered from the shelf to the rise, during Plio-Pleistocene glacial and interglacials, and representing unique records of processes from which we can study the ice sheet dynamics and variations in oceanic circulation. At Site U1524, most laminae are graded consistently with turbidity current deposition, whereas at Site U1525, laminae character is highly variable, and many contain sharp upper and lower contacts consistent with reworking/sediment winnowing by bottom currents. Despite the near complete sediment recovery in the piston cored intervals of Sites U1524 and U1525, the occurrence of hiatuses, low carbonate content, and highly reworked diatom material in some intervals hampers a confident detailed correlation between the sites (McKay et al., 2019a). The discovery of a well-preserved tephra layer in Site U1524 allows identifying intervals of interest in other cores from the Ross Sea to carry out ultra-high resolution geochemical and physical properties investigations and locate cryptotephra levels in sediment core records between the Ross Sea and the Amundsen Sea. The identification of cryptotephra layers would enable core-to-core correlations of past changes in ocean-ice interactions along the Pacific coastline of Antarctica.

Site U1524 was drilled on the continental rise (74°13.05'S, 173°37.98'W, 2394 m water depth) on the south-eastern levee of the Hillary Canyon (Figure 1), one of the largest conduits of dense shelf water delivery from the Antarctic continental shelf into the abyssal ocean where it forms the Antarctic Bottom Water (AABW). The scientific target for the deep-drilling site was the recovery of sediments of channel-overspill and drift deposits. It recovered a high-resolution Plio-Pleistocene turbidite record related to the cascading of Ross Sea Bottom Water (RSBW) down the Hillary Canyon, feeding the AABW, thus providing a reconstruction of this critical component of the global oceanic overturning circulation over much of the past ~3.3 Ma (McKay et al., 2019a, 2019b, 2019c,

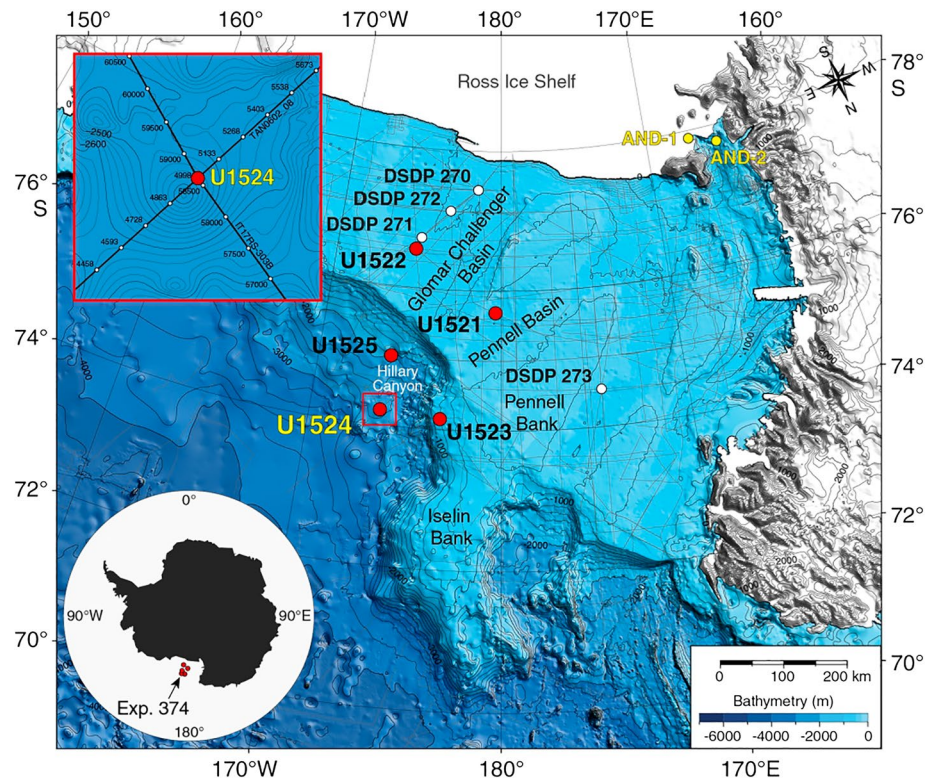


Figure 1. Bathymetric map of the Ross Sea area from IBCSO (Arndt et al., 2013). Locations of Site U1524 and the other sites from International Ocean Discovery Program (IODP) Expedition 374 sites are indicated with red dots. Nearby DSDP Leg 28 Sites 270–273 (white dots), and The Antarctic DRILLing Project (ANDRILL) Cores AND-1 and AND-2 (yellow dots) are also shown. In the red inset, the map with Site U1524 is reported. The figure is redrawn from McKay et al. (2019b).

2019d). The ANtarctic DRILLing Project (ANDRILL) Site AND-1B previously recovered an exceptional Plio-Pleistocene record of ice sheet fluctuation over the continental shelf, alongside volcanic activity in the McMurdo Sound region (Naish et al., 2009). Correlation to that site will allow for an unprecedented link between continental shelf processes and changing AABW flux into the deep ocean through this period. The overspill turbidites at Site U1524 are interbedded with periods of pelagic deposition that will enable proxy reconstructions of surface and bottom water properties and of circulation strength changes.

Site U1524 consists of three drill holes (U1524A, B, and C) at 2394 m water depth, with the deepest core recovered to a depth of 441.9 m below the seafloor at Hole U1524C and comprises upper Miocene to Pleistocene sediments (Figure 2). Based on shipboard core description, the sequences were lithologically divided into three main units (I–III) each further sub-divided into subunits that mainly comprise diatom-bearing mud, diatom-rich mud, diatom ooze, sandy mud, and muddy diamictite (Figure 2). In general, the facies architecture and assemblage of sequences recovered from the sites indicate pelagic sedimentation and re-deposition via turbidity currents (graded mm-scale silt/sand laminae), with a lesser influence of alongslope current reworking (McKay et al., 2019a). Uppermost lithostratigraphic Unit I consists of ~200 m of sediments dated to the late Pliocene to Pleistocene and includes unconsolidated massive to laminated diatom-bearing/rich mud interbedded with muddy diatom ooze (Figure 2). Unit I is subdivided into three subunits (IA, IB, and IC). Subunit IA consists of ~78 m of massive to laminated diatom-bearing to diatom-rich mud interbedded at the decimeter to meter scale with diatom-bearing/rich mud to sandy mud with dispersed clasts. Sand laminae and lenses are increasingly abundant toward the base of the unit (Figure 2). A 20 cm-thick tephra layer (afterward named U1524 tephra) occurs in the core Section 6H-2A between 44.19 and 43.99 m core depth below the seafloor, method A (CSF-A), hereafter referred to as m below the seafloor (mbsf) (Figure 2). The tephra has a sharp and irregular base, displays weak normal grading, and the upper boundary is gradational into overlaying mud (Figure 2). It is also located between two paleomagnetic reversals at 39.775 ± 0.125 mbsf and 61.415 ± 1.185 mbsf, interpreted during shipboard measurement to

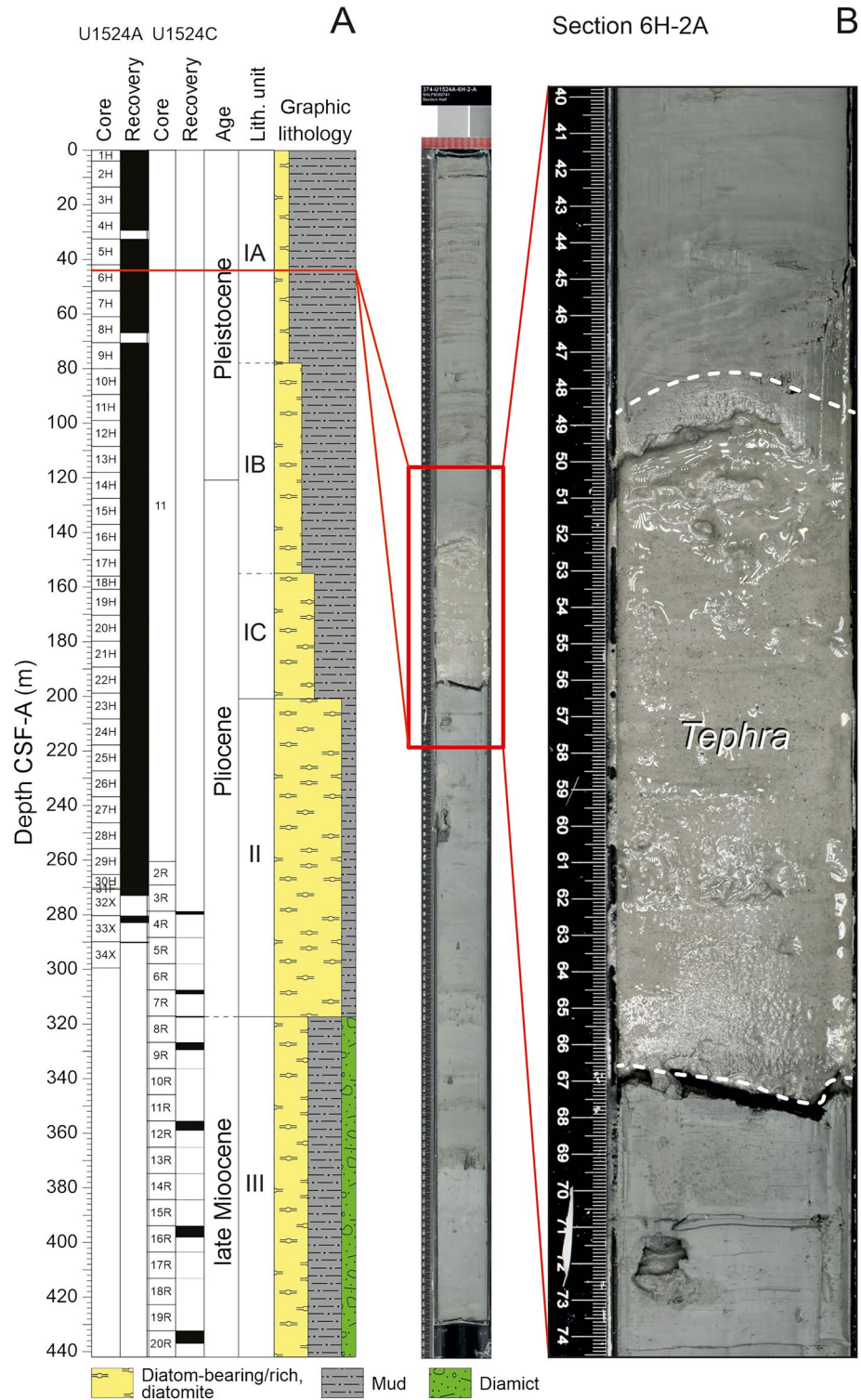


Figure 2. (a) Lithostratigraphic column for Site U1524 with the position of studied tephra layer highlighted. (b) Core photographs of Section 374-U1524A-6H-2A and detail of the rhyolite tephra studied in this work. The scale is in cm.

represent the base of the Cobb Mountain chron (1.221 Ma) and top of the Olduvai chron (1.775 Ma), respectively (McKay et al., 2019b). Consequently, this tephra provides an important chronological constraint for Site U1524.

3. Methods

Bulk tephra samples were described under a petrography microscope. Grain size analyses were carried out at one- ϕ intervals from 0 to 6 ϕ ($\phi = -\log_2 D$, where D is the particle diameter in millimeters) using mechanical dry sieving. The main sedimentological parameters were calculated according to Inman (1952). Grain size fraction $>250 \mu\text{m}$ was embedded using epoxy resin and polished for the analyses. A scanning electron microscope (SEM) Zeiss EVO 10 MA at the Istituto Nazionale di Geofisica e Vulcanologia, Sezione di Pisa (INGV-Pisa) laboratories was used to describe volcanic textures, and an Oxford Si(Li) energy-dispersive X-ray detector (EDS) was also used to determine mineral phase compositions.

Major-element analyses of mineral and glass samples were undertaken on a JEOL JXA 8230 electron probe microanalyzer (EPMA) at Victoria University of Wellington using wavelength dispersive spectrometry techniques. Operating conditions were 15 kV with 8 nA with a defocused 10- μm beam for glass with reduced count times for Na to minimize alkali loss. Calibrated international standards including ATHO-G, T1-G (Jochum et al., 2006), and VG-568 (USNM 72854) were analyzed as unknowns to monitor instrumental drift as well as the precision and accuracy of the analyses. Approximate 2 SD precisions calculated from repeated analyses of calibrated standards are generally <5 relative % for oxides that occur in concentrations of >1 wt% (Data Set S1). The trace-element concentrations were determined on single glass shards by Laser Ablation Inductively Coupled Plasma-Mass Spectrometry (LA-ICP-MS) at the Università di Perugia, Dipartimento di Fisica e Geologia. The analyses were carried out with a Teledyne Photon Machine G2 laser ablation system coupled to a Thermo Fisher Scientific iCAP-Q, quadrupole based, ICP-MS (Petrelli et al., 2008; 2016a; 2016b). The LA-ICP-MS operating conditions were optimized before each analytical session by continuous ablation of NIST SRM 612 glass reference material (Pearce et al., 1997) to provide maximum signal intensity and stability for the ions of interest while suppressing oxides formation (ThO^+/Th^+ below 0.5%). The U/Th ratio was also monitored and maintained close to 1. The stability of the system was evaluated on ^{139}La , ^{208}Pb , ^{232}Th , and ^{238}U by a short-term stability test. It consisted of 5 acquisitions (one minute each) on a linear scan of NIST SRM 612 glass reference material (Petrelli et al., 2016a; 2016b). Tephra glasses were analyzed by using a circular laser beam with a diameter of 20 or 30 μm , a frequency of 10 Hz, and an energy density at the sample surface of 3.5 J/cm². NIST SRM 610 reference material (Pearce et al., 1997) was used as the calibrator and ^{29}Si as the internal standard. USGS BCR2G reference material was analyzed as unknown to provide quality control (Jochum et al., 2005). Under these operating conditions, precision and accuracy are better than 10% for all the investigated elements (Petrelli et al., 2008; 2016a; 2016b) (Data Set S2).

Separation of sanidine grains $>250 \mu\text{m}$ was obtained by densimetric separation using heavy liquids (lithium heteropolytungstates) diluted at 2.65 g/cm³ at INGV-Pisa sedimentology laboratory. Quartz crystals were separated from sanidine by handpicking.

^{40}Ar - ^{39}Ar analyses of sanidine extracted from the tephra layer were completed at IGG-CNR (Pisa). The separate (grain size $\geq 250 \mu\text{m}$) was leached in an ultrasonic bath at room temperature for a few minutes in diluted HF (7%) and was then wrapped in aluminum foil and irradiated for 8 h in the core of the TRIGA reactor at the University of Pavia (Italy) along with the monitor Alder Creek sanidine (ACs). Single grains of alkali feldspar were placed into 1.5-mm diameter holes whereas multigrain fractions were spread onto the bottom of 3- or 6-mm diameter holes of copper holders, loaded into a vacuum chamber comprising a laser port consisting of a ZnSe window fitted with a differentially pumped flange, and baked for 12 h at 150°C. Total fusion experiments were performed using a CO₂ laser beam (New Wave Research MIR10–30 CO₂ laser system) defocused to a ~ 1 mm spot size. Step-heating experiments were completed on 3 multigrain aliquots, ranging in weight from ~ 3 to ~ 8 mg, with the laser beam defocused to 2-mm spot size and slowly rastered over the samples. Steps were carried out at increasing laser power until complete melting. Extracted gases were purified in a low volume stainless steel inlet system for 4 min (including 30 s of lasering), using three SAES NP10 getters (one, water-cooled, held at $\sim 400^\circ\text{C}$ and two at room temperature). Ar isotope measurements were performed simultaneously in static mode using an ARGUS VI™ (Thermo Fisher Scientific) multicollector mass spectrometer. ^{36}Ar was measured using a Compact Discrete Dynode (CDD) detector and the remaining Ar isotopes using Faraday detectors, equipped with $10^{12} \Omega$ resistors

for ^{40}Ar and ^{38}Ar and $10^{13} \Omega$ resistors for ^{39}Ar and ^{37}Ar . Faraday detectors were cross-calibrated for the slight offset with $\sim 3,000$ fA air shots. The CDD was calibrated daily for its yield by measuring four to six air pipettes before the first analysis. Mass discrimination was determined through an automated pipette system before and after samples analyses and ranged from 1.00153 ± 0.00012 to 1.00293 ± 0.00010 atomic mass unit ($\pm 1\sigma$). Blanks were monitored generally every two runs and were subtracted from succeeding sample results (Data Set S3). Based on the daily reproducibility of line blanks, a minimum uncertainty of 1% and 2% were applied to masses ^{40}Ar and ^{36}Ar , respectively. The correction factors for interfering isotopes from K and Ca were based on determinations on K-rich and Ca-rich glasses (uncertainties $\pm 1\sigma$): $(^{40}\text{Ar}/^{39}\text{Ar})_{\text{K}} = 0.00982 \pm 0.00021$ ($^{38}\text{Ar}/^{39}\text{Ar}$) $_{\text{K}} = 0.01266 \pm 0.00013$ ($^{39}\text{Ar}/^{37}\text{Ar}$) $_{\text{Ca}} = 0.000697 \pm 0.000022$ and $(^{36}\text{Ar}/^{37}\text{Ar})_{\text{Ca}} = 0.000266 \pm 0.000021$. Uncertainties on total gas ages, on error-weighted mean ages and on ages derived from isochron plots also include the uncertainty in the fluence monitor and are given at 2σ . Ages were calculated relative to an ACs age of 1.1848 Ma (Niespolo et al., 2017), using decay constants recalculated by Min et al. (2000) and an atmospheric $^{40}\text{Ar}/^{36}\text{Ar}$ ratio of 298.56 ± 0.31 (Lee et al., 2006). Ar isotope concentrations are reported in Data Set S3 as relative abundances and have been corrected for blank, mass discrimination, and radioactive decay. More details about mass spectrometer calibration and analysis can be found in Di Vincenzo et al. (2021).

4. Results

4.1. Texture, Mineral Assemblage, and Glass Geochemistry

As mentioned above the tephra has a sharp and irregular base and the upper boundary is gradational into overlaying mud (Figure 2). Tephra consists of massive and faint laminated, very well-sorted, very fine ash ($Md\phi = 3.15$, $\sigma\phi = 0.97$). Particles forming the tephra layer span the entire range of shapes and vesicularity and include (a) highly vesicular, frothy vesicular near-clear to light gray-greenish <1 mm pumice fragments (Figures 3a and 3b), (b) fibrous pumice fragments with tubular vesicles (Figures 3c and 3d), and (c) platy glass shard with flat surfaces, y-shaped shards and blocky shards (Figures 3c and 3d). In general, the glass fragments are microlite-free except for rare, $<100 \mu\text{m}$ sanidine and quartz microlites (Figures 3e and 3f). The tephra contains abundant euhedral to subhedral crystals of sanidine and quartz $<500 \mu\text{m}$ (mean size $<250 \mu\text{m}$). Rare, $<500 \mu\text{m}$ crystals of amphiboles occur and in particular euhedral crystals of aenigmatite, and anhedral often reabsorbed crystals of an amphibole belonging to the arfvedsonite-riebeckite series. Crystals of Fe-Ti oxide (ilmenite) and apatite of a few microns also occur (Figure 3). Lithic fragments are rare and consist of granite, dark holocrystalline volcanic rocks, and altered tuffs.

Glass shards have a very homogeneous rhyolite composition (Figure 4) with an average $\text{SiO}_2 = 74.87$ wt. % (± 0.18 , SD), $\text{K}_2\text{O} + \text{Na}_2\text{O} = 9.45$ wt. % (± 0.22 , SD). Their peralkalinity indices ($\text{P.I.} = [\text{mol}(\text{Na} + \text{K})/\text{Al}]$) range from 0.93 to 1.32, and glasses plot across the border between the comendite and pantellerite fields in the classification diagram of MacDonald (1974) (Figure 5). FeO and CaO contents are 4.33 wt. % (± 0.17 SD) and 0.19 wt. % (± 0.01 SD), respectively. No significant variations occur in other major and minor oxides. Average major, minor (recalculated to 100 wt. % anhydrous) and trace element glass compositions are reported in Table 1, and the full geochemical data set is reported in Data Set S1 and S2.

Figure 5 reports the primordial mantle normalized diagram (McDonough & Sun, 1995) for a large number (i.e., 27) of trace elements for the studied U1524 tephra and the range of the LA-ICP-MS analyses reported as vertical error bar. Based on Figure 5, it emerges that trace elements in the U1524 tephra are enriched by a factor of ca. 50–100 to the primordial mantle. As a general trend, it is possible to observe a continuous decrease in the enrichment values by progressively passing from Cs to Lu. Exceptions are Ba, Sr, Eu, and Ti, highlighting negative anomalies when compared with the other trace elements. In details, Eu is enriched by a factor of ~ 10 , Ba and Ti values are in agreement with primordial mantle values, and Sr is depleted by a factor of ~ 7 (Figure 5).

4.2. ^{40}Ar - ^{39}Ar Geochronology: Results and Interpretation

A total of 49 grains, corresponding approximately to ~ 2 mg of sanidine separate, were individually analyzed by the total fusion technique. Given the small grain size of the mineral separate (mostly around a few hundreds of micrometers in size), the step-heating technique was not applied on individual grains. Total fusion data yielded ages defining a relatively wide and significant age interval, ranging at face value from ~ 1.24 to ~ 1.44 Ma, and characterized by a nearly continuous variation (Figure 6a). Even excluding the two analyses yielding the

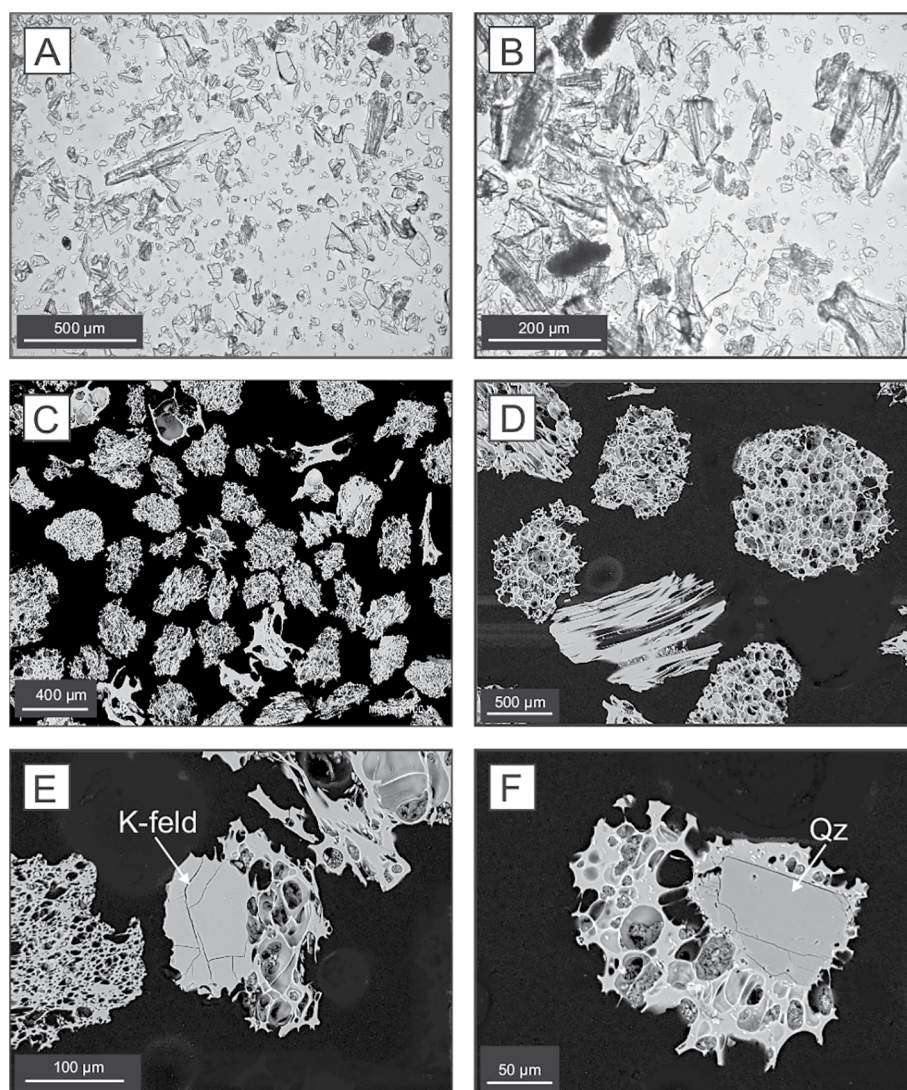


Figure 3. Optical and Scanning Electron Microscope (SEM) images of the studied tephra. (a–b) optical microscope photographs of glass shard textures with poorly vesicular blocky glass shards, cusped and platy bubble wall, and pumiceous clast with tubular vesicles (c–d) SEM images of pumiceous moderate to highly vesicular pumice fragments with foamy to tubular texture. (e) pumice fragments including a subhedral ca. 100 μm microlites of sanidine and (f) quartz.

oldest ages (>1.4 Ma), the probability that data belong to the same population of ages is less than 0.001. The cumulative probability plot (Figure 6a) reveals discernible peaks at ~ 1.28 , 1.32, 1.35, and 1.43 Ma. However, the 26 youngest age data are indistinguishable within analytical uncertainties and yield a weighted mean age of 1.2826 ± 0.0080 Ma ($\pm 2\sigma$ -MSWD, mean squared of weighted deviates, of 1.35, probability of 0.11). In a $^{36}\text{Ar}/^{40}\text{Ar}$ versus $^{39}\text{Ar}/^{40}\text{Ar}$ isochron diagram (Figure S1), these data yield a regression line (MSWD = 1.4, probability 0.09) with an intercept age of 1.282 ± 0.012 Ma and a $^{40}\text{Ar}/^{36}\text{Ar}$ y-intercept of 302 ± 21 . The overall grain to grain heterogeneity in age revealed by total fusion analysis of individual grains may arise from true sample heterogeneity, due to a diachronous population of grains and/or to heterogeneous distribution of excess Ar (parentless ^{40}Ar) hosted in fluid and/or in melt inclusions and producing meaningless older ages. Alternatively, in light of the small sizes of the grains investigated and of the consequent small ion beams analyzed, the scatter could also arise from inaccurate blank correction and consequently from underestimated uncertainties.

In order to clarify the causes of inter-grain age heterogeneity revealed by the total fusion technique, three aliquots consisting of some milligrams of sanidine separate were analyzed through the laser step-heating technique. All the three experiments gave internally discordant age profiles (Figure 6b), with anomalously old ages at low and

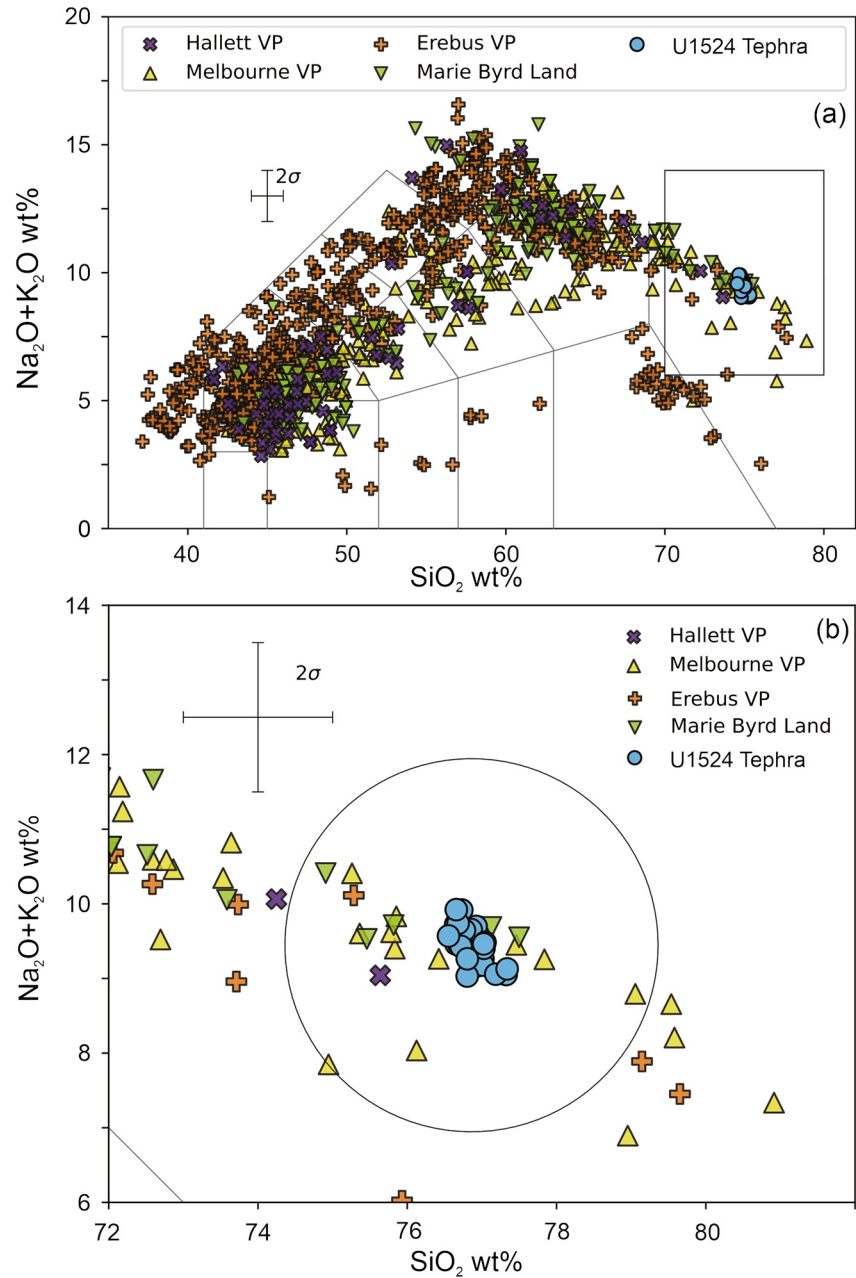


Figure 4. (a) Total alkali versus silica plot (after LeBas et al., 1986) showing the composition of the studied tephra. All data are normalized to anhydrous compositions. (b) Inset of the total alkali versus silica plot showing the narrow compositional range of the U1524 tephra in comparison to other regional tephra. Geochemical data: Hallett Volcanic Province (VP) - Aviado et al. (2015); Harrington et al. (1967); Hamilton (1972); Kyle (1990); Hornig and Wörner (1991); Mortimer et al. (2007); Nardini et al. (2009); Panter et al. (2018); Rocholl et al. (1995). Melbourne VP: Armienti and Tripodo (1991); Armienti et al. (1991); Beccaluva et al. (1991); Hornig and Wörner (1991); Kim et al. (2019); Kyle (1982, 1986, 1990); Müller et al. (1991); Nardini et al. (2009); Noll (1985); Worner et al. (1989); Rocchi and Smellie (2021). Rocholl et al. (1995). Erebus VP: Aviado et al. (2015); Cooper et al. (2007); Ellerman and Kyle (1990); Forbes and Kuno (1965); Goldich et al. (1975); Iacovino (2014); Kelly et al. (2008); Kyle (1976, 1990); Kyle et al. (1979); Lee et al. (2015); LeMasurier and Thomson (1990); Martin et al. (2010; 2013); Muncy (1979); Phillips et al. (2018); Rasmussen et al. (2017); Scanlan (2008); Stuckless and Ericksen (1976); Sullivan (2006); Timms (2006); Wright-Grassham (1987).

high [only for aliquots (2) and (3)] temperatures. The minimum of the saddle is defined by: a single step in aliquot (a), yielding an age of 1.306 ± 0.004 Ma ($\pm 2\sigma$); two consecutive steps in aliquot (b), yielding a mean age of 1.2997 ± 0.0041 Ma ($\pm 2\sigma$); four consecutive steps in aliquot (3), yielding a mean age of 1.3009 ± 0.0029 Ma

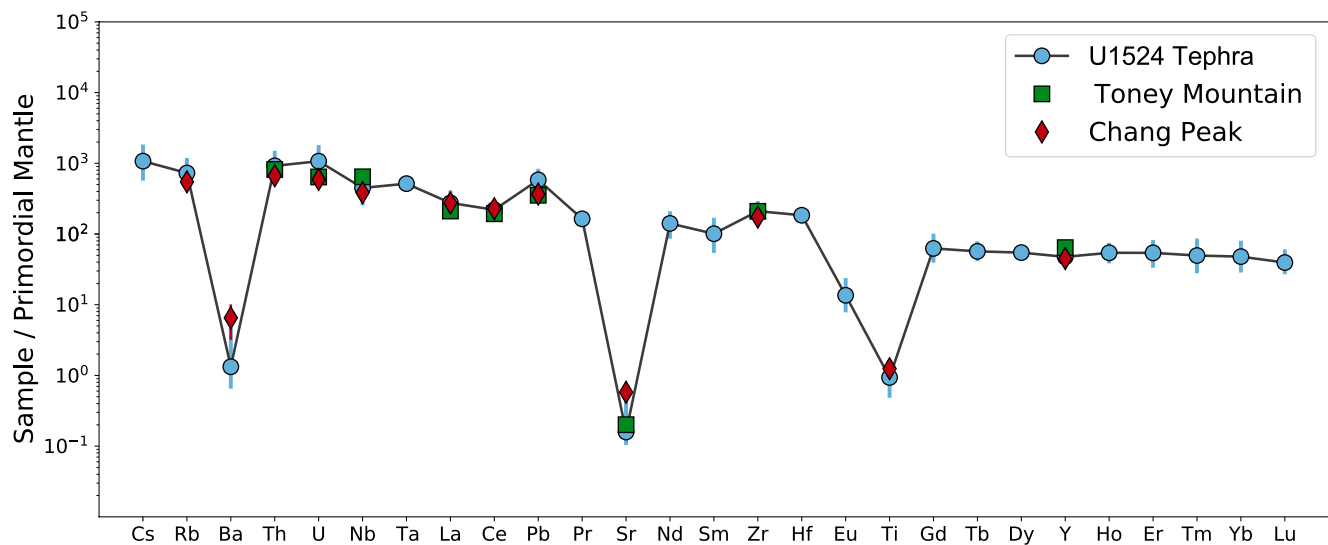


Figure 5. Primordial mantle normalized (after McDonough & Sun, 1995) trace element profile of mean glass composition of U1524 tephra. The full range of the analyses is reported as vertical error (blue bar). Representative trace elements analyses from Chang Peak (samples 32 and 32A) and Toney Maintain (sample 76D) samples are also reported for comparison. Data from LeMasurier and Thomson (1990).

($\pm 2\sigma$). Saddle-shaped age spectra like those obtained from step-heating experiments from the present study may be diagnostic of excess Ar, likely hosted in fluid inclusions (e.g., Esser et al., 1997; Lanphere & Darlymple, 1976; Wartho et al., 1996), with the implication that conservatively speaking, the minima of the saddle should be taken as maximum age estimates. In light of (a) ^{40}Ar - ^{39}Ar results from single-grain total fusion analyses, (b) the lack of a positive correlation between radiogenic Ar contents and ages, (c) the shape of the age spectra derived from step-heating analyses and (d) the inter-grain chemical homogeneity revealed by SEM-EDS chemical data, we concluded that sanidine crystals are heterogeneously contaminated by an excess Ar component, likely hosted in fluid inclusions, and we consider the isochron age of 1.282 ± 0.012 Ma derived from data of the youngest sanidine grains our best estimate for the age of U1524A tephra.

5. Discussion

Features of the U1524A tephra such as stratigraphic relationships with embedded sediments, thickness, sedimentological features, volcanic particle morphology, the extremely homogeneous geochemical composition, and absence of detrital material indicate that this layer is primary and was likely deposited by fallout during an eruption of considerable intensity. The ^{40}Ar - ^{39}Ar age determined on sanidine crystals in the tephra is 1.2842 ± 0.012 Ma and is in excellent agreement with the paleomagnetic age data. In fact, the core (6H) where the tephra was found, is chronologically constrained between two paleomagnetic ages of 1.221 Ma at 39.775 mbsf (4.315 m above the tephra), and 1.775 Ma at 61.415 mbsf (c. 17 m below the tephra), respectively (McKay et al., 2019a). Based purely on the interpolation of a linear sedimentation rate of 36.49 m/Ma, using these paleomagnetic constraints, the age at ~44.09 mbsf (midpoint of the tephra) is calculated at c. 1.3 Ma. This age is highly consistent with the ^{40}Ar - ^{39}Ar age, and also provides a tie-point to help constrain a subtle increase in sedimentation rate downcore, which is also consistent with a general downcore increase in sedimentation rate in Site U1524 through the late Pliocene to Pleistocene (McKay et al., 2019a).

5.1. Origin of U1524 Tephra

Site U1524A is at least 500–700 km away from the volcanoes of the Hallett, Erebus, and Melbourne Volcanic Provinces of the McMurdo Volcanic Group and c. 1,000–1,700 km away from volcanoes of the Marie Byrd Land volcanic province (Figure 7). Even if the tephra could be slightly overthickened a rather high-intensity Plinian explosive eruption is necessary to produce an ash layer with this thickness, grain size, and overall sedimentological features at such a considerable distance from these sources and in such deep waters. For these reasons, the volcanic source for the studied tephra was searched among those volcanoes of the Erebus, Melbourne, Hallett,

Table 1
Representative Major and Trace Elements Glass Composition From the U1524 Tephra, Chang Peak and Toney Mountain Samples

U1524 tephra			Chang peak			Toney mountain
WDS			32A	32	32A (glass)	76D
XRF			XRF	XRF	WDS	XRF
<i>n</i>	40	st.dev (2σ)	12			
SiO ₂	74.86	0.18	71.69	72.8	72.32	72.26
TiO ₂	0.17	0.01	0.25	0.18		0.16
Al ₂ O ₃	10.59	0.08	10.79	10.62	9.00	12.54
FeO ₁	4.33	0.17	4.62	3.76	5.32	1.87
MnO	0.07	0.02	0.10	0.06		1.70
MgO	0.003	0.005	2.04	0.11		0.07
CaO	0.19	0.01	0.77	0.22		0.09
Na ₂ O	5.33	0.19	5.51	5.01	4.58	0.27
K ₂ O	4.12	0.11	4.56	4.38	4.57	6.11
P ₂ O ₅			0.02			4.21
Cl	0.34	0.01			0.24	0.02
LOI			0.56			0.42
Total	100.00		100.91	97.14	96.04	99.72
LA-ICP-MS						
<i>n</i>	103	st.dev (2σ)				
Li	185	34				
Be	20	3				
Sc	17	3				
V			4	5		7
Cr			9	0		6
Co			3	0		0
Ni			8	3		8
Cu	5	2	7	0		4
Zn			358	273		396
Ga	45	9	37	35		44
Rb	438	76	315	341		420
Sr	3	1	13	10		4
Y	204	8	217	170		13
Zr	2209	213	2086	1,557		2198
Nb	295	42	286	219		424
Cs	23	4				
Ba	9	3	64	22		12
La	178	25	214	142		137
Ce	369	21	473	291		324
Pr	42	2				
Nd	176	22				
Sm	41	7				
Eu	2.1	0.4				

and Marie Byrd Land volcanic provinces, which were active during the middle-late Pleistocene, had deposits compatible with a Plinian-type eruption and a rhyolitic composition. An extra-Antarctic origin of the tephra (e.g., New Zealand or southern South American volcanoes) is highly unlikely due to the relevant grain size and thickness of the tephra layer. For example, the ash from the Oruanui supereruption from Taupo (25,580 ± 258 cal. a BP) recently identified in the WDC06A ice core from central West Antarctica, has particles <20–30 μm in diameter and occur in the form of thin cryptotephra (Dunbar et al., 2017). This shows that even the largest class of non-Antarctic volcanic explosive eruption is capable of delivering only fine-grained particles with relatively low concentration in geologic records of Antarctica. Conversely, the possibility that the volcanic source that produced the tephra is no longer visible, dismantled and/or covered by ice cannot be ruled out. We have compared the composition of tephra glass with the composition of Quaternary (Pleistocene) volcanic rock from the Erebus, Melbourne, Hallett, and Marie Byrd Land volcanic provinces and with tephra found in Antarctic ice cores, marine sediments, blue ice, and continental outcrops in Antarctica (database published by Del Carlo et al., 2018).

Rocks with rhyolitic compositions are quite rare in Antarctica. No rhyolitic products have been erupted during the Pleistocene by volcanoes of the Hallett, Erebus, and Melbourne Volcanic Province of the McMurdo Volcanic Group. Rhyolites have been erupted only by Mount Morning of the Erebus Volcanic Province during the earlier, mildly alkaline eruptive phase and crop out at Castle and Gandalf Ridge and Pinnacle Valley (Martin et al., 2010). However, these products have been dated by ⁴⁰Ar/³⁹Ar at 15.4 ± 0.1 Ma (sample OU 78508 of Martin et al., 2010) and thus are considerably older than the tephra layer studied here. Similarly, in the Melbourne Volcanic Province rhyolite rocks have been produced in the Malta Plateau volcanic complex (Hornig et al., 1991; Müller et al., 1991; Rocholl et al., 1995), at Mount Noice in the Mount Rittmann complex (Armienti & Tripodo, 1991), and Mount Overlord (Noll, 1985). Rhyolite at Malta Plateau yields K-Ar ages older than c. 6.7 Ma (Müller et al., 1991), and peralkaline rhyolites on the Mount Overlord Complex are as old as c. 7.2 Ma, obtained from four K-Ar dates (Armstrong, 1978), thus again they are much older than the age of the U1524 tephra layer.

The Marie Byrd Land volcanic province includes 18 major volcanic centers that have been active since c. 34 Ma (Rocchi et al., 2006) and, among these Mount Siple (2.0–0.0 Ma), Mount Berlin (2.7–0.1 Ma), Mount Moulton (3.9–1.0 Ma), Mount Waesche (2.0–1.1 Ma), Boyd Ridge (2.7–1.0 Ma), and Mount Frakes (1.6–0.03 Ma) have been active in the considered time interval (Paulsen & Wilson, 2010). Rhyolite is a rare occurrence also in the Marie Byrd Land Volcanic Province and crops out at Chang Peak volcano (comendite glass and comendite vitrophyre samples 32 and 32A; LeMasurier & Thomson, 1990), at Toney Mountain (comendite vitrophyre 76D; LeMasurier & Thomson, 1990), at Ames Range (pantellerite AR42A; LeMasurier et al., 2011), at Mount Hartigan (comendite and rhyolite 43A and 47; LeMasurier & Rex, 1989), and Mount Moulton (pantellerite 2A, 67-2A). Among these, only comendite samples at Toney Mountain and Chang Peak are compatible in age with the U1524 tephra. The first has a K-Ar age of 1 ± 0.2 Ma (LeMasurier & Thomson, 1990) and the second is dated at 1.6 ± 0.2 Ma using the K-Ar method (sample 32A of LeMasurier & Rex, 1989). Recently, ⁴⁰Ar-³⁹Ar analyses were determined on single sanidine crystals from rare rhyolite exposures at Chang Peak and Mount Waesche

Table 1
Continued

	U1524 tephra		Chang peak			Toney mountain
			32A	32	32A (glass)	76D
	WDS		XRF	XRF	WDS	XRF
<i>n</i>	40	st.dev (2σ)	12			
Gd	34	6				
Tb	5.6	0.6				
Dy	37	2				
Ho	8.1	0.8				
Er	24	3				
Tm	3	0.6				
Yb	21	4				
Lu	3	0.4				
Hf	52	3				
Ta	19	1				
Pb	87	10	57	53		53
Th	73	12	55	51		65
U	22	4	13	11		13

volcanic centers. They yielded an age of 1.315 ± 0.007 Ma for a pumice sample MB.7.3 (prior-published age of 1.6 ± 0.2 Ma, sample 32A of LeMasurier & Rex, 1989), and of 1.385 ± 0.003 Ma for a second sample (MB.8.1) consisting of a porphyritic cryptocrystalline lava (Iverson et al., 2021).

From a geochemical perspective, the major element glass composition of rhyolites from Mount Toney and Chang Peak volcanoes is very similar to that of U1524 tephra. As shown in Figure 5, the available trace elements signature for Chang Peak and Toney Mountain both have a similar composition to that of the U1524 tephra. Figure 8 shows binary diagrams for selected trace elements (i.e., Th, Y, Nb, and Ce that are available for both Chang Peak and Toney Mountain), plotted against Zr (taken as differentiation index) from a vast array of available literature for the Hallett, Erebus, Melbourne, and Marie Byrd Land Volcanic Provinces (Armienti & Tripodo, 1991; Armienti et al., 1991; Aviado et al., 2015; Beccaluva et al., 1991; Cooper et al., 2007; Ellerman & Kyle, 1990; Forbes & Kuno, 1965; Goldich et al., 1975; Hamilton 1972; Harrington et al., 1967; Hart et al., 1997; Hole & LeMasurier 1994; Hornig & Wörner, 1991; Iacovino 2014; Kelly et al., 2008; Kim et al., 2019; Kyle 1976, 1982, 1986, 1990; Kyle et al., 1979; Lee et al., 2015; LeMasurier & Thomson 1990; LeMasurier et al., 2011, 2018; Martin et al., 2010, 2013, Mortimer et al., 2007; Müller et al., 1991; Muncy 1979; Nardini et al., 2009; Noll 1985; Panter et al., 1997, 2000, 2018; Phillips et al., 2018; Rasmussen et al., 2017; Rocchi & Smellie, 2021; Rocholl et al., 1995; Scanlan 2008; Stuckless & Ericksen, 1976; Sullivan 2006; Timms 2006; Worner et al., 1989; Wright-Grassham, 1987). The trace element distribution diagrams highlight that the U1524 tephra is at the extreme bound for incompatible trace element enrichments in the investigated compositions but in good statistical agree-

ment with the few data available for Chang Peak. The Toney Mountain trace element signature is also in statistical agreement with the U1524 tephra (Figures 5 and 8) with the exceptions being Nb and Y which are slightly more enriched than the U1524 tephra.

Some differences exist between the mineralogy of the U1524 tephra and comendite vitrophyre 76D of Mount Toney. The comendite sample at Mount Toney contains phenocrysts of alkali feldspar and brown amphibole but no quartz is reported. This sample should be discarded as a potential proximal counterpart because the U1524 tephra is rich in quartz. Conversely, Chang Peak samples include an aphyric comendite pumice (32) and a comenditic vitrophyre (32A) bearing phenocrysts of quartz, alkali feldspar, ilmenite, and aenigmatite (LeMasurier & Thomson, 1990). The Chang Peak volcano samples are described in LeMasurier and Thomson (1990). These are retrieved from the only two existing exposures, both on the caldera rim and both offering only a limited range of sampling that consist of a massive, saccharoidal rhyolite, and a coarse-grained Plinian fall deposit formed of weakly lithified rhyolitic pumice (LeMasurier & Rex, 1989; LeMasurier & Thomson, 1990).

Based on major and trace elements glass compositions, petrographic features, and age, the sample that represents the best candidate for the proximal deposit of the tephra studied here is the 32A rhyolite (or MB.7.3 of Iverson et al., 2021) sampled on the caldera rim of Chang Peak volcano. Note, however, that ^{40}Ar - ^{39}Ar data reported by Iverson et al. (2021) are in a meeting abstract, and consequently a more rigorous comparison with our Ar data from the U1524 tephra is currently precluded.

The volcanic structure of the Chang Peak volcano also agrees well with the occurrence of a high-magnitude Plinian eruption such as the one that generated the marine tephra. The Chang Peak volcano is truncated by a 10-km-wide caldera. This type of volcanic structure forms under various tectono-magmatic conditions but is often associated with catastrophic ignimbrite-forming explosive events (Acocella 2007). We thus suggest that the U1524 tephra may be the distal fallout deposits of a Calabrian age major caldera-forming eruption at Chang Peak volcano, 1.282 ± 0.012 Ma ago. Volcanic activity resumed in the same area approximately at c. 1 Ma, c. 0.3 Ma later, with the formation of Mount Waesche shield volcano that lies on the south rim of Chang Peak volcano (LeMasurier & Thomson, 1990) and possibly continued until recent times (Le Masurier, 1972).

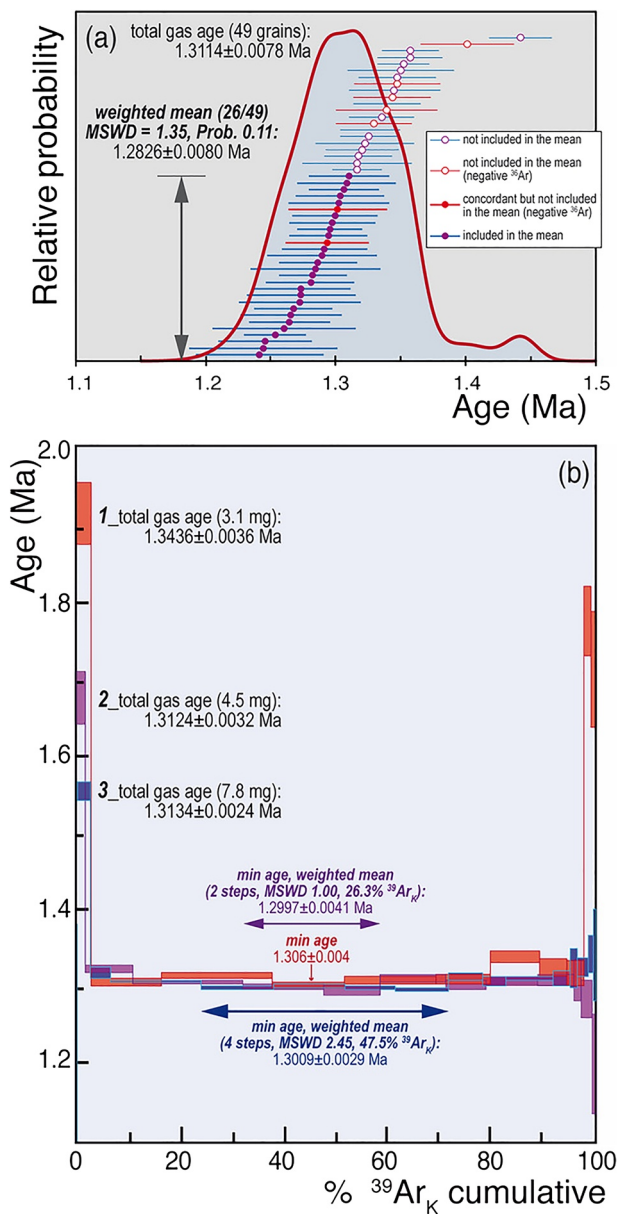


Figure 6. (a) Cumulative probability and ranked distribution of ^{40}Ar - ^{39}Ar ages from total fusion experiments on individual sanidine grains. Bars are 2σ analytical uncertainties. (b) Age release spectra of three multigrain aliquots of alkali feldspar. Box heights indicate the 2σ analytical uncertainty.

5.2. Paleoenvironmental Significance of U1524 Tephra

Given the thickness of this tephra (20 cm), it ought to be present in other sediments and possibly in deep ice core records in the area; however, so far it has not been identified at other drilling sites.

Coeval sediment is eroded at many sites on the Ross Sea continental shelf, including IODP Site U1521 (McKay et al., 2019a), DSDP Sites 270–273 (Hayes & Frakes, 1975), Cape Roberts Project Sites CRP-1 and CPR-2/2A, and ANDRILL Site AND-1B (Naish et al., 2009). At IODP Site U1522, recovery was only 11.5% over the 200-m interval dated to the Pleistocene, so even if the tephra was deposited at the location, it was not recovered during coring operations. Site U1523 is located on the outer continental shelf on the southeastern flank of Iselin Bank; in the sediments recovered at this site, between 19 and 33 cm in the U1523A-3H-1 core section (corresponding to 18.19–18.33 m CSF-A), clear glass shards and pumiceous fragments occur mixed with foraminifers, diatoms, and silt/clay particles. This volcanoclastic layer shows signs of reworking (e.g. erosive base, mud chips, etc.) but the XRF core logger data signature is similar to that of the U1524 tephra, which shows Si and Zr enrichment and Ba and Ti depletion. The age of this interval is also broadly compatible (early Pleistocene) with that of U1524 tephra (McKay et al., 2019c). We thus argue that the volcanoclastic layer at Site U1523 could be the reworked counterpart of U1524 tephra.

Site U1525 is located upslope of Site U1524 on the southeastern levee of Hillary Canyon. Despite being in a similar depositional setting, there is no evidence of the tephra at this site. While recovery is very good, it is possible that the tephra is present in the sediment at this site but fell within a gap between cores and so was not recovered. Sediment at Site U1523 and U1525 also shows evidence of reworking by bottom currents (McKay et al., 2019d) so it is possible that the tephra may have been deposited but then removed via these currents. Unfortunately, this hampered the correlation between the different drilling sites and also the more detailed reconstruction of tephra dispersal and deposit parameters that would have been useful in reconstructing source eruption volcanic parameters and eruption dynamics. A careful check of sediment geochemical composition at Site U1525 will potentially reveal the occurrence of dispersed volcanoclastic materials and cryptotephra with composition matching with that of U1524 tephra and will be targeted in future work.

Conversely, since tephra grains are transported as suspended particles by winds, the tephra dispersal could help reconstruct past climatic conditions and in particular past atmospheric circulation patterns of Antarctica (Narcisi et al., 2005). The identification of such thick tephra at Site U1524, west of the inferred source in the Marie Byrd Land, is indicative of westward atmospheric circulation at the moment of the tephra dispersal. Atmospheric near-surface winds from ERA5 reanalysis (Hersbach et al., 2020) show that part of the ash produced in the Chang Peak volcanic eruption in the Marie Byrd Land that falls toward the surface can be transported and deposited at Site U1524 (Figure 9). During the austral summer, Easterly winds, blowing westward, provide two different atmospheric transport pathways, (a) a southward branch through Siple Coast, and (b) a northward branch along Mary Byrd Land coastal area, both sustained by katabatic winds (Figure 9a). This second pathway almost contracts during austral winter when Westerlies strengthen and Easterlies shift toward Antarctica (Figure 9b). Westward atmospheric flow is consistent with Mezgec et al. (2017) back trajectory analysis showing that particles from the Western Ross Sea could end up on the East Antarctic plateau. Last Glacial Maximum (LGM, c. 21 ka) and Last Great Interglacial (LIG, peak at ~127 ka) atmospheric circulation (Figure S2) show that ash transport from the Marie Byrd Land to Site U1524 could occur in a similar way today.

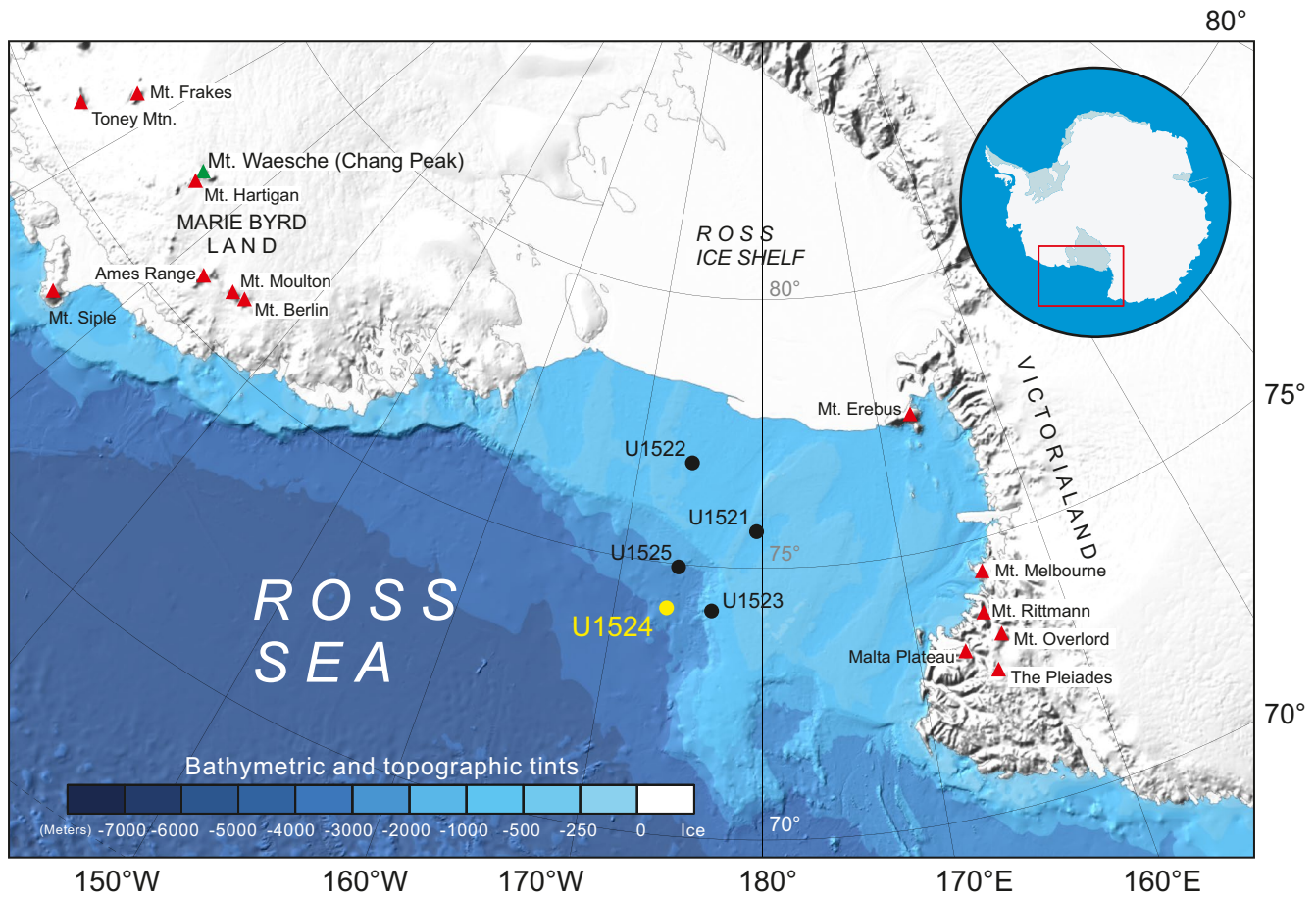


Figure 7. Bathymetric map of the Ross Sea area with included sites drilled during the International Ocean Discovery Program (IODP) Expedition 374 and main volcanic structure discussed in the text (red triangles) and Chang Peak volcano (green triangle). Ross Sea bathymetry is from the International Bathymetric Chart of the Southern Ocean (Arndt et al., 2013).

Sea ice drift is another way to indirectly convey ash from the Amundsen Sea to the Ross Sea. The ice drift is wind-driven and the winter cyclonic conditions that develop over the Amundsen Sea are favorable to a westward coastal sea ice drift toward the Ross Sea (Figure 9b.). However, the occurrence of sea ice would mostly prevent direct deposition of ash through the water column at a particular site and cannot explain the primary characters of the studied tephra (thickness, structure, etc) at Site U1524. Therefore, we suggest that the tephra deposition occurred during a warming phase when sea ice was seasonal and the ice sheet grounding line likely retreated southward from the continental shelf edge. Thus, most of the tephra could have been deposited during austral summer when Easterlies blew from Marie Byrd Land to the Ross Sea. We argue a predominately atmospheric transport pathway, with minimal evidence of substantial reworking by ocean currents. In fact, after the rapid fall out of the heavy ash load, across the upper water layers (with relatively high-speed westward Antarctic Slope Current), the ash settled down to the sea-floor and was not reworked because the currents bottom velocity is almost null at Site U1524. However, localized oceanic currents or vertical plume processes (see Manville & Wilson, 2004) could act to focus sedimentation and enhance the thickness of the tephra layer at Site U1524. The plume mechanism implies a large volume of tephra, originated from a highly explosive eruption, transported westward from the Marie Byrd Land, and deposited rapidly as fall-out settling at Site U1524. This hypothesis fits well with the tephra geochemical and sedimentological interpretations. At other sites, this tephra may be dispersed over a wider area directly by oceanic bottom currents reworking. In the future, the U1524 tephra could be of critical importance to compare and correlate the timing of climatic fluctuation between the continental and marine realms. From the perspective of future deep ice drillings aimed at recovering ice records up to 1.5 million years old ice (see Beyond EPICA project), or from “snaphot” records of multimillion-year-old from horizontal ice cores from blue ice areas (c.f.

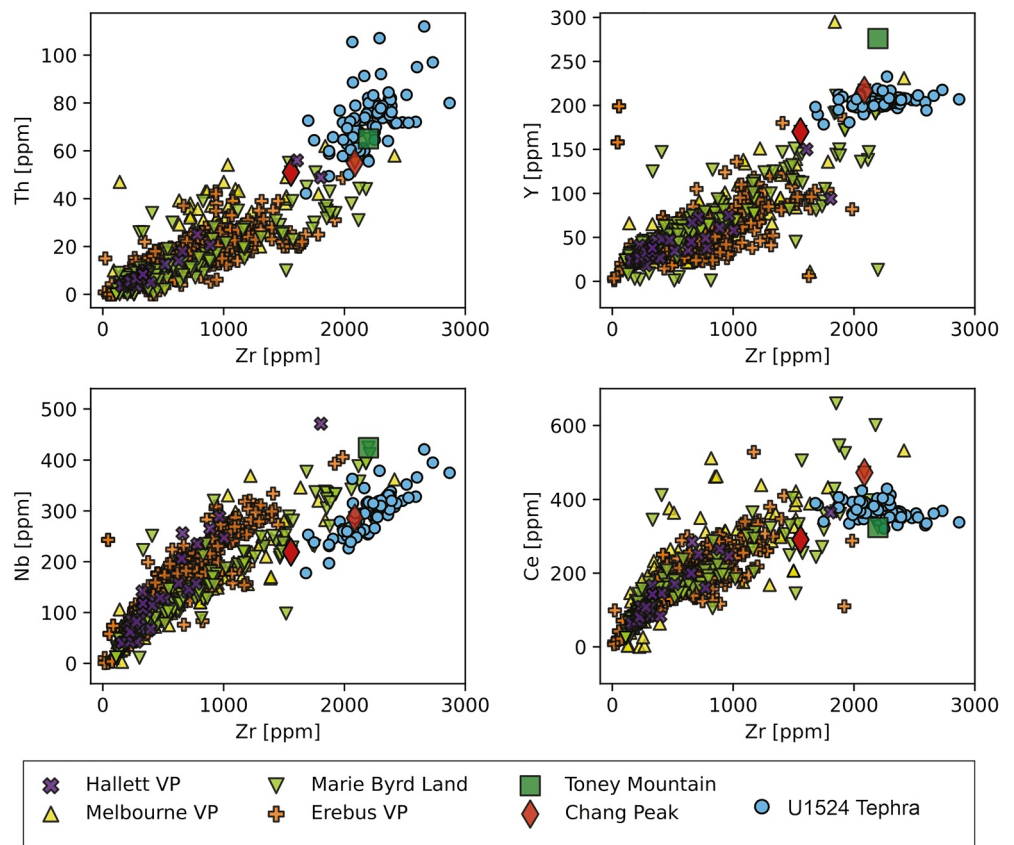


Figure 8. Binary variation diagrams for selected trace elements (Th, Y, Nb, and Ce) plotted against Zr, taken as differentiation index of U1524 tephra compared to trace elements composition compared of volcanic rocks available for Erebus, Hallett, Melbourne, and Marie Byrd land (see Figure 4 for data references) volcanic provinces including Chang Peak (red diamond) and Toney Mountain rocks (green square).

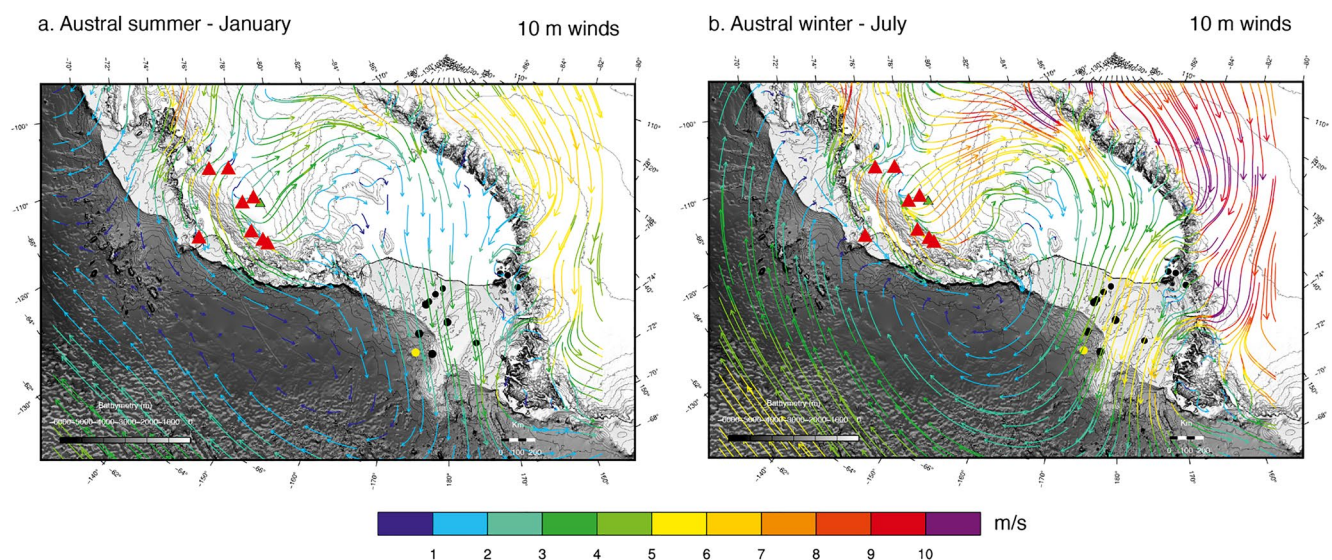


Figure 9. Near-surface winds (10 meters) circulation averaged over 2000–2019 for (a) January (peak of austral summer) and (b) July (peak of austral winter). Color scale corresponds to the 10-m wind speed in m/s. Bathymetry is from IBCSO (Arndt et al., 2013) and ice sheet surface elevation is from BedMap2 (Fretwell et al., 2013). Black dots indicate IODP Exp. 374 sites, DSDP drilling sites and ANDRILL sites as of Figure 1. Site U1524 is shown in yellow and Chang Peak is shown as a green triangle.

Yan et al., 2019), the tephra could offer an exceptional possibility of dating and of synchronizing ice sequences with the marine environment.

6. Conclusion

We report a discrete, lower Pleistocene rhyolitic tephra layer found at 43.99 mbsf intercalated in the sedimentary sequence recovered at Site U1524 during IODP Expedition 374, in the Ross Sea. The geochemical composition including the peralkaline nature of the volcanic glass and the high iron content, point to an origin from volcanoes of Western Antarctica and more precisely from the Marie Byrd Land region. ^{40}Ar - ^{39}Ar data, based on both single grain total fusion analyses and multigrain step-heating analyses on sanidine crystals extracted from the tephra, suggest an eruption age of 1.282 ± 0.012 Ma, which is consistent with the paleomagnetic age constraints of Site U1524. By integrating petrographic and geochemical data with age constraints we correlated this tephra to rhyolitic Plinian fallout deposits exposed on the rim of the 10-km-wide Chang Peak caldera volcano, in the Marie Byrd Land, as far as c. 1,300 km from Site U1524.

Our findings represent one of the few cases in which a marine tephra layer is correlated with reasonable certainty to its source volcano in Antarctica, offering important volcanological data on the (a) the eruptive history of the poorly known Chang Peak alkaline volcano in Marie Byrd Land, (b) the intensity of the eruption that generated it and (c) the potential impact of such major eruptions on Antarctic ice sheet.

This tephra provides an important chronological marker for the early Pleistocene in the Ross Sea area considering its far-traveled nature and thickness. It, therefore, represents a critical marker to correlate and synchronize coeval records of the Ross Sea, the neighboring Amundsen Sea, and the Western Antarctica continental records. In fact, because the tephra was deposited far from the volcanic source both in the continental and deep marine realms it can be used as a key horizon to synchronize and correlate paleoclimatic records resulting in a better understanding of the synchronicity/asynchronicity between marine and terrestrial climate change in Antarctica.

From the perspective of future deep ice drillings aimed at recovering ice records up to 1.5 million years old (see Beyond EPICA project), or snapshot ice cores records of ancient ice from blue ice areas, the tephra offers an exceptional possibility of precisely and independently dating the continental ice sequences and of synchronizing them with records from the marine environment.

Data Availability Statement

Major-element data of single glass shards (Data Set S1) are available at <https://doi.pangaea.de/10.1594/PANGAEA.933364>. The trace-element concentrations including the analysis of the USGS BCR2G standard used to provide the instrument quality control at <https://doi.org/10.1594/PANGAEA.933481> (Data Set S2). ^{40}Ar - ^{39}Ar total fusion data are available at <https://doi.org/10.1594/PANGAEA.933421> (Data Set S3).

References

- Abbott, P.M., Griggs, A.J., Bourne, A.J., & Davies, S.M. (2018). Tracing marine cryptotephra in the North Atlantic during the last glacial period: Protocols for identification, characterisation and evaluating depositional controls. *Marine Geology*, 401, 81–97. <https://doi.org/10.1016/j.margeo.2018.04.008>
- Acocella, V. (2007). Understanding caldera structure and development: An overview of analogue models compared to natural calderas. *Earth-Science Reviews*, 85(3–4), 125–160. <https://doi.org/10.1016/j.earscirev.2007.08.004>
- Armienti, P., Civetta, L., Innocenti, F., Manetti, P., Tripodo, A., Villari, L., & Vita, G. (1991). New petrological and geochemical data on Mt. Melbourne Volcanic Field, Northern Victoria Land, Antarctica (II Italian Antarctic Expedition). *Memorie Della Societa Geologica Italiana*, 46, 397–424.
- Armienti, P., & Tripodo, A. (1991). Petrography and chemistry of lavas and comagmatic xenoliths of Mt. Rittmann, a volcano discovered during the IV Italian expedition in Northern Victoria Land (Antarctica). *Memorie Della Societa Geologica Italiana*, 46, 427–451.
- Armstrong, R. L. (1978). K-Ar dating: Late Cenozoic McMurdo volcanic group and dry valley glacial history, Victoria Land, Antarctica. *New Zealand Journal of Geology and Geophysics*, 21(6), 685–698. <https://doi.org/10.1080/00288306.1978.10425199>
- Arndt, J. E., Schenke, H.W., Jakobsson, M., Nitsche, F. O., Buys, G., Goleby, B., et al. (2013). The International Bathymetric Chart of the Southern Ocean (IBCSO) Version 1.0—A new bathymetric compilation covering circum-Antarctic waters. *Geophysical Research Letters*, 40, 3111–3117. <https://doi.org/10.1002/grl.50413>
- Aviador, K. B., Rilling-Hall, S., Bryce, J. G., & Mukasa, S. B. (2015). Submarine and subaerial lavas in the West Antarctic Rift System: Temporal record of shifting magma source components from the lithosphere and asthenosphere. *Geochemistry, Geophysics, Geosystems*, 16(12), 4344–4361. <https://doi.org/10.1002/2015GC006076>

Acknowledgments

The authors would like to thank the two reviewers S.C. Kuehn and M. Jutzeler for very helpful suggestions and improvements of the manuscript. Christine Smith Siddoway and John Smellie are greatly acknowledged for their helpful comments and the discussion about the tephra provenance. This research used data and samples provided by the International Ocean Discovery Program (IODP). ADR and BS were funded by Italian Programma Nazionale di Ricerche in Antartide (PNRA), 2016/A3 00055 project, FC by PNRA18_00002 and LD by PNRA16_00016 project. DK was supported by the IODP JOIDES Resolution Science Operator and US National Science Foundation (Grant 1326927). RM was funded by the Royal Society Te Apārangi NZ Marsden Fund (Grant 18-VUW-089). The Ar laser probe facility was realized with the financial support of Consiglio Nazionale delle Ricerche (CNR). This paper is sponsored by the SCAR Expert Group, AntVolc. Open Access Funding provided by Istituto Nazionale di Geofisica e Vulcanologia within the CRUI-CARE Agreement.

- Beccaluva, L., Coltorti, M., Orsi, G., Saccani, E., Siena, F., Colleoni, F., et al. (1991). Nature and evolution of subcontinental lithospheric mantle of Antarctica: Evidence from ultramafic xenoliths of the Melbourne volcanic province (northern Victoria Land, Antarctica). *Memorie della Società Geologica Italiana*, Past continental shelf evolution increased Antarctic ice sheet sensitivity to climatic conditions. *Scientific Reports*, *46*, 353–370. <https://doi.org/10.1038/s41598-018-29718-7>
- Cooper, A. F., Adam, L. J., Coulter, R. F., Eby, G. N., & McIntosh, W. C. (2007). Geology, geochronology and geochemistry of a basanitic volcano, White Island, Ross Sea, Antarctica. *Journal of Volcanology and Geothermal Research*, *165*, 189–216. <https://doi.org/10.1016/j.jvolgeores.2007.06.003>
- Curzio, P., Folco, L., Ada Laurenzi, M., Mellini, M., & Zeoli, A. (2008). A tephra chronostratigraphic framework for the Frontier Mountain blue-ice field (northern Victoria Land, Antarctica). *Quaternary Science Reviews*, *27*, 602–620. <https://doi.org/10.1016/j.quascirev.2007.11.017>
- Davies, S. M. (2015). Cryptotephra: The revolution in correlation and precision dating. *Journal of Quaternary Science*, *30*(2), 114–130. <https://doi.org/10.1002/jqs.2766>
- Del Carlo, P., Di Roberto, A., Di Vincenzo, G., Bertagnini, A., Landi, P., Pompilio, M., et al. (2015). Late Pleistocene-Holocene volcanic activity in northern Victoria Land recorded in Ross Sea (Antarctica) marine sediments. *Bulletin of Volcanology*, *77*, 1–17. <https://doi.org/10.1007/s00445-015-0924-0>
- Del Carlo, P., Di Roberto, A., D'Orazio, M., Petrelli, M., Angioletti, A., Zanchetta, G., et al. (2018). Late Glacial-Holocene tephra from southern Patagonia and Tierra del Fuego (Argentina, Chile): A complete textural and geochemical fingerprinting for distal correlations in the Southern Hemisphere. *Quaternary Science Reviews*, *195*, 153–170. <https://doi.org/10.1016/j.quascirev.2018.07.028>
- Di Roberto, A., Albert, P. G., Colizza, E., Del Carlo, P., Di Vincenzo, G., Gallerani, A., et al. (2020). Evidence for a large-magnitude Holocene eruption of Mount Rittmann (Antarctica): A volcanological reconstruction using the marine tephra record. *Quaternary Science Reviews*, *250*, 106629. <https://doi.org/10.1016/j.quascirev.2020.106629>
- Di Roberto, A., Colizza, E., Del Carlo, P., Petrelli, M., Finocchiaro, F., & Kuhn, G. (2019). First marine cryptotephra in Antarctica found in sediments of the western Ross Sea correlates with englacial tephra and climate records. *Scientific Reports*, *9*, 10628. <https://doi.org/10.1038/s41598-019-47188-3>
- Di Roberto, A., Del Carlo, P., & Pompilio, M. (2021). Marine record of Antarctic volcanism from drill cores. In J. Smellie, K. Panter, & A. Geyer (Eds.), *Volcanism in Antarctica: 200 million years of subduction, rifting and continental break-up* (Vol. 55, pp. 631–647). Geological Society. <https://doi.org/10.1144/M55-2018-49>
- Di Vincenzo, G., Folco, L., Suttle, M. D., Brase, L., & Harvey, R. P. (2021). Multi-collector $^{40}\text{Ar}/^{39}\text{Ar}$ dating of microtektites from Transantarctic Mountains (Antarctica): A definitive link with the Australasian tektite/microtektite strewn field. *Geochimica et Cosmochimica Acta*, *298*, 112–130. <https://doi.org/10.1016/j.gca.2021.01.046>
- Dunbar, N. W., Iverson, N. A., Van Eaton, A. R., Sigl, M., Alloway, B. V., Kurbatov, A. V., et al. (2017). New Zealand supereruption provides time marker for the Last Glacial Maximum in Antarctica. *Scientific Reports*, *7*, 12238. <https://doi.org/10.1038/s41598-017-11758-0>
- Dunbar, N. W., Zielinski, G. A., & Voisins, D. T. (2003). Tephra layers in the siple dome and Taylor dome ice cores, Antarctica: Sources and correlations. *Journal of Geophysical Research*, *108*, 2374. <https://doi.org/10.1029/2002JB002056>
- Ellerman, P. J., & Kyle, P. R. (1990). Beaufort Island. In W. E. LeMasurier, & J. W. Thomson (Eds.), *Volcanoes of the antarctic plate and southern oceans, antarctic research series* (Vol. 48, pp. 80–161). American Geophysical Union.
- Esser, R. P., McIntosh, C. W., Heizler, M. T., Kyle, P. R., (1997). Excess argon in melt inclusions in zero-age anorthoclase feldspar from Mt. Erebus, Antarctica, as revealed by the 39 and 40 of $^{39}\text{Ar}/^{40}\text{Ar}$. *Geochimica et Cosmochimica Acta*, *61*, 3789–3801. [https://doi.org/10.1016/S0016-7037\(97\)00287-1](https://doi.org/10.1016/S0016-7037(97)00287-1)
- Forbes, R. B., & Kuno, H. (1965). The regional petrology of peridotite inclusions and basaltic hostrocks. *Proceedings upper mantle symposium* (pp. 80–161).
- Fretwell, P., Pritchard, H. D., Vaughan, D. G., Bamber, J. L., Barrand, N. E., Bell, R., et al. (2013). Bedmap2: Improved ice bed, surface and thickness datasets for Antarctica. *The Cryosphere*, *7*, 375–393. <https://doi.org/10.5194/tc-7-375-2013>
- Goldich, S., Treves, S., Suhr, N., & Stuckless, J. (1975). Geochemistry of the Cenozoic volcanic rocks of Ross Island and vicinity, Antarctica. *The Journal of Geology*, *83*, 415–435. <https://doi.org/10.1086/628120>
- Hamilton, W. (1972). *The Hallett volcanic province, Antarctica*. United States Geological Survey, Geological Survey Professional Paper.
- Harpel, C. J., Kyle, P. R., & Dunbar, N. W. (2008). Englacial tephrostratigraphy of Erebus volcano, Antarctica. *Journal of Volcanology and Geothermal Research*, *177*, 549–568. <https://doi.org/10.1016/j.jvolgeores.2008.06.001>
- Harrington, H. J., Wood, B. L., McKellar, I. C., & Lensen, G. J. (1967). Topography and geology of the Cape Hallett district, Victoria Land, Antarctica. *New Zealand Geological Survey Bulletin*, *80*, 1–100.
- Hart, S. R., Blusztajn, J., LeMasurier, W. E., & Rex, D. C. (1997). Hobbs Coast Cenozoic volcanism: Implications for the West Antarctic rift system. *Chemical Geology*, *139*, 223–248. [https://doi.org/10.1016/S0009-2541\(97\)00037-5](https://doi.org/10.1016/S0009-2541(97)00037-5)
- Hayes, D. E., and Frakes, L. A. (1975). General synthesis, Deep Sea drilling Project Leg 28. In A. G. Kaneps (Ed.), *Initial reports of the Deep Sea drilling Project*. 28. <https://doi.org/10.2973/dsdp.proc.28.1975>
- Hersbach, H., Bell, B., Berrisford, P., Hirahara, S., Horányi, A., Muñoz-Sabater, J., et al. (2020). The ERA5 global reanalysis. *Quarterly Journal of the Royal Meteorological Society*, *146*, 1999–2049. <https://doi.org/10.1002/qj.3803>
- Hillenbrand, C.-D., Moreton, S. G., Caburlotto, A., Pudsey, C. J., Lucchi, R. G., Smellie, J. L., et al. (2008). Volcanic time-markers for Marine Isotopic Stages 6 and 5 in Southern Ocean sediments and Antarctic ice cores: Implications for tephra correlations between paleoclimatic records. *Quaternary Science Reviews*, *27*, 518–540. <https://doi.org/10.1016/j.quascirev.2007.11.009>
- Hole, M. J., & LeMasurier, W. E. (1994). Tectonic controls on the geochemical composition of Cenozoic, mafic alkaline volcanic rocks from West Antarctica. *Contributions to Mineralogy and Petrology*, *117*, 187–202. <https://doi.org/10.1007/BF00286842>
- Hornig, I., & Wörner, G. (1991). Zirconolite-bearing ultra-potassic veins in a mantle-xenolith from Mt. Melbourne Volcanic Field, Victoria Land, Antarctica. *Contribution to Mineralogy and Petrology*. *106*, 355–366. <https://doi.org/10.1007/BF00324563>
- Hornig, I., Wörner, G., & Zipfel, J. (1991). Lower crustal and mantle xenoliths from the Mt. Melbourne Volcanic Field, Northern Victoria Land, Antarctica. *Memorie Della Società Geologica Italiana*, *46*, 337–352.
- Iacovino, K. (2014). An unexpected journey: Experimental insights into magma and volatile transport beneath Erebus volcano, Antarctica (Doctoral dissertation). <https://doi.org/10.17863/CAM.16442>
- Inman, D. L. (1952). Measures for describing the size distribution of sediments. *Journal of Sedimentary Petrology*, *22*, 125–145. <https://doi.org/10.1306/D42694DB-2B26-11D7-8648000102C1865D>
- Iverson, N., Siddoway, C., Zimmerer, M., Smellie, J., Dunbar, N., & Gohl, K. (2021). *Rhyolite volcanism in the Marie Byrd Land volcanic province, Antarctica: New evidence for pyroclastic eruptions during latest Pliocene icesheet expansion*. <https://doi.org/10.5194/egusphere-egu21-9003>
- Jochum, K. P., Pfänder, J., Woodhead, J. D., Willbold, M., Stoll, B., Herwig, K., et al. (2005). MPI-DING glasses: New geological reference materials for in situ Pb isotope analysis. *Geochemistry, Geophysics, Geosystems*, *6*(10). <https://doi.org/10.1029/2005GC000995>

- Jochum, K. P., Stoll, B., Herwig, K., Willbold, M., Hofmann, A. W., Amini, M., et al. (2006). MPI-DING reference glasses for in situ microanalysis: New reference values for element concentrations and isotope ratios. *Geochemistry, Geophysics, Geosystems*, 7, Q02008. <https://doi.org/10.1029/2005GC001060>
- Kelly, P. J., Kyle, P. R., Dunbar, N. W., & Sims, K. W. W. (2008). Geochemistry and mineralogy of the phonolite lava lake, Erebus volcano, Antarctica: 1972–2004 and comparison with older lavas. *Journal of Volcanology and Geothermal Research*, 177(3), 589–605. <https://doi.org/10.1016/j.jvolgeores.2007.11.025>
- Keys, J. R., Anderton, P. W., & Kyle, P. R. (2017). Tephra and debris layers in the Skelton Neve And Kempe Glacier, South Victoria Land, Antarctica. *New Zealand Journal of Geology and Geophysics*, 20(5), 971–1002. <https://doi.org/10.1080/00288306.1977.10420692>
- Kim, J., ParkLee, J. W. M. J., Lee, J. I., Kyle, P. R., & Kyle, P. R. (2019). Evolution of alkalic magma systems: Insight from coeval evolution of sodic and potassic fractionation lineages at The Pleiades volcanic complex, Antarctica. *Journal of Petrology*, 60(1), 117–150. <https://doi.org/10.1093/petrology/egy108>
- Kyle, P. R. (1976). *Geology, mineralogy, and geochemistry of the late Cenozoic McMurdo Volcanic Group (Doctoral dissertation)*. Retrieved from Victoria University Research Archive. <http://hdl.handle.net/10063/510>
- Kyle, P. R. (1982). Volcanic geology of The Pleiades, Northern Victoria Land, Antarctica. In C. Craddock (Ed.), *Antarctic geosciences* (pp. 747–754). University of Wisconsin Press.
- Kyle, P. R. (1986). Mineral chemistry of late Cenozoic McMurdo volcanic group from the Pleiades, northern Victoria Land. *Antarctic Research Series* (Vol. 46, pp. 305–337). American Geophysical Union. <https://doi.org/10.1029/ar046p0305>
- Kyle, P. R., Adams, J., & Rankin, P. C. (1979). Geology and petrology of the McMurdo Volcanic Group at Rainbow Ridge, Brown Peninsula, Antarctica. *Geological Society of America, Bulletin*, 90(7), 676–688. [https://doi.org/10.1130/0016-7606\(1979\)90%3C676:GAPOTM%3E2.0.CO;2](https://doi.org/10.1130/0016-7606(1979)90%3C676:GAPOTM%3E2.0.CO;2)
- Kyle, P. R., McIntosh, W. C., Schmidt-Thomé, M., Mueller, P., Tessensohn, F., Noll, M. R., et al. (1990). McMurdo Volcanic Group Western Ross Embayment. In W. E. LeMasurier, J. W. Thompson, P. E. Baker, J. W. Kyle, P. D. Rowley, J. L. Smellie & W. J. Verwoerd et al. (Eds.), *Volcanoes of the antarctic plate and southern oceans* (Vol. 48, pp. 18–145). <https://doi.org/10.1029/AR048p0018>
- Lane, C. S., Lowe, D. J., Blockley, S. P. E., Suzuki, T., & Smith, V. C. (2017). Advancing tephrochronology as a global dating tool: Applications in volcanology, archeology, and paleoclimatic research. *Quaternary Geochronology*, 40, 1–7. <https://doi.org/10.1016/j.quageo.2017.04.003>
- Lanphere, M. A., & Dalrymple, G. B. (1976). Identification of Excess ⁴⁰Ar by the ⁴⁰Ar/³⁹Ar age spectrum technique. *Earth and Planetary Science Letters*, 32(2), 141–148. [https://doi.org/10.1016/0012-821X\(76\)90052-2](https://doi.org/10.1016/0012-821X(76)90052-2)
- LeBas, M. J. L., Maitre, R. W. L., Streckeis, A., & Zanettin, B. (1986). A chemical classification of volcanic rocks based on the total alkali-silica diagram. *Journal of Petrology*, 27(3), 745–750. <https://doi.org/10.1093/petrology/27.3.745>
- Lee, J.-Y., Marti, K., Severinghaus, J. P., Kawamura, K., Yoo, H.-S., Lee, J. B., & Kim, J. S. (2006). A redetermination of the isotopic abundances of atmospheric Ar. *Geochimica et Cosmochimica Acta*, 70(17), 4507–4512. <https://doi.org/10.1016/j.gca.2006.06.1563>
- Lee, M. J., Lee, J. I., Kim, T. H., Lee, J., & Nagao, K. (2015). Age, geochemistry and Sr-Nd-Pb isotopic compositions of alkali volcanic rocks from Mt. Melbourne and the western Ross Sea, Antarctica. *Geosciences Journal*, 19, 681–695. <https://doi.org/10.1007/s12303-015-0061-y>
- LeMasurier, W. E. (1972). Marie Byrd Land Quaternary volcanism: Byrd ice core correlations and possible climatic influences. *Antarctic Journal*, 7, 139–141.
- LeMasurier, W. E., Choi, S. H., Kawachi, Y., Mukasa, S. B., & Rogers, N. W. (2011). Evolution of pantellerite-trachyte-phonolite volcanoes by fractional crystallization of basanite magma in a continental rift setting, Marie Byrd Land, Antarctica. *Contributions to Mineralogy and Petrology*, 162, 1175–1199. <https://doi.org/10.1007/s00410-011-0646-z>
- LeMasurier, W. E., Choi, S. H., Kawachi, Y., Mukasa, S. B., & Rogers, N. W. (2018). Dual origins for pantellerites, and other puzzles, at Mount Takaha volcano, Marie Byrd Land, West Antarctica. *Lithos*, 296–299, 142–162. <https://doi.org/10.1016/j.lithos.2017.10.014>
- LeMasurier, W. E., & Rex, D. C. (1989). Evolution of linear volcanic ranges in Marie Byrd land, West Antarctica. *Journal of Geophysical Research*, 94(B6), 7223–7236. <https://doi.org/10.1029/JB094iB06p07223>
- Lowe, D. J. (2011). Tephrochronology and its application: A review. *Quaternary Geochronology*, 6(2), 107–153. <https://doi.org/10.1016/j.quageo.2010.08.003>
- MacDonald, R. (1974). Nomenclature and petrochemistry of the peralkaline oversaturated extrusive rocks. *Bulletin Volcanologique*, 38, 498–516. <https://doi.org/10.1007/BF02596896>
- Manville, V., & Wilson, C. J. N. (2004). Vertical density currents: A review of their potential role in the deposition and interpretation of deep-sea ash layers. *Journal of the Geological Society*, 161, 947–958. <https://doi.org/10.1144/0016-764903-067>
- Martin, A. P., Cooper, A. F., & Dunlap, W. J. (2010). Geochronology of Mount Morning, Antarctica: Two-phase evolution of a long-lived trachyte-basanite-phonolite eruptive center. *Bulletin of Volcanology*, 72, 357–371. <https://doi.org/10.1007/s00445-009-0319-1>
- Martin, A. P., Cooper, A. F., & Price, R. C. (2013). Petrogenesis of Cenozoic, alkalic volcanic lineages at Mount Morning, West Antarctica and their entrained lithospheric mantle xenoliths: Lithospheric versus asthenospheric mantle sources. *Geochimica et Cosmochimica Acta*, 122(1), 127–152. <https://doi.org/10.1016/j.gca.2013.08.025>
- Masson-Delmotte, V., Stenni, B., Pol, K., Braconnot, P., Cattani, O., Falourd, S., et al. (2010). EPICA Dome C record of glacial and interglacial intensities. *Quaternary Science Reviews*, 29(1–2), 113–128. <https://doi.org/10.1016/j.quascirev.2009.09.030>
- McDonough, W. F., & Sun, S. S. (1995). Composition of the Earth. *Chemical Geology*, 120, 223–253. [https://doi.org/10.1016/0009-2541\(94\)00140-4](https://doi.org/10.1016/0009-2541(94)00140-4)
- McKay, R. M., DeSantis, L., Kulhanek, D. K., Ash, J. L., Beny, F., Brownie, I. M., et al. (2019a). Ross Sea West Antarctic ice sheet history. *Proceedings of the International Ocean Discovery Program* (Vol. 374). International Ocean Discovery Program. <https://doi.org/10.14379/iodp.proc.374.2019>
- McKay, R. M., DeSantis, L., Kulhanek, D. K., Ash, J. L., Beny, F., Brownie, I. M., et al. (2019b). Site U1524. In R. M. McKay, L. De Santis, & D. K. Kulhanek (Eds.), *The expedition 374 scientists, Ross Sea West Antarctic ice sheet history. Proceedings of the International Ocean discovery program* (Vol. 374). International Ocean Discovery Program. <https://doi.org/10.14379/iodp.proc.374.106.2019>
- McKay, R. M., DeSantis, L., Kulhanek, D. K., Ash, J. L., Beny, F., Brownie, I. M., et al. (2019c). Site U1523. In R. M. McKay, L. De Santis, D. K. Kulhanek, (Eds.), *Expedition 374 scientists proceedings of the International Ocean discovery program* (Vol. 374). <https://doi.org/10.14379/iodp.proc.374.105.2019>
- McKay, R. M., DeSantis, L., Kulhanek, D. K., Ash, J. L., Beny, F., Brownie, I. M., et al. (2019d). Site U1525. In R. M. McKay, L. De Santis, D. K. Kulhanek, & the (Eds.), *Expedition 374 scientists proceedings of the International Ocean discovery program* (Vol. 374). <https://doi.org/10.14379/iodp.proc.374.107.2019>
- Mezgec, K., Stenni, B., Crosta, X., Masson-Delmotte, V., Baroni, C., Braida, M., et al. (2017). Holocene sea ice variability driven by wind and polynya efficiency in the Ross Sea. *Nature Communications*, 8, 1334. <https://doi.org/10.1038/s41467-017-01455-x>
- Min, K., Mundil, R., Renne, P. R., & Ludwig, K. R. (2000). A test for systematic errors in ⁴⁰Ar/³⁹Ar geochronology through comparison with U/Pb analysis of a 1.1-Ga rhyolite. *Geochimica et Cosmochimica Acta*, 64, 73–98. [https://doi.org/10.1016/S0016-7037\(99\)00204-5](https://doi.org/10.1016/S0016-7037(99)00204-5)

- Moreton, S. G., & Smellie, J. L. (1998). Identification and correlation of distal tephra layers in deep-sea sediment cores, Scotia Sea, Antarctica. *Annals of Glaciology*, 27, 285–289. <https://doi.org/10.3189/1998AoG27-1-285-289>
- Mortimer, N., Dunlap, W. J., Isaac, M. J., Sutherland, R. P., & Faure, K. (2007). Basal Adare volcanics, Robertson Bay, North Victoria Land, Antarctica: Late Miocene intraplate basalts of subaqueous origin. *United States geological survey open-file report, 2007-1047*.
- Müller, P., Schmidt-Tomè, M., Kreuzer, H., Thessensohn, F., & Vetter, U. (1991). (Vol. XLVI, pp. 315–336). *Memorie della Società Geologica Italiana. Cenozoic peralkaline magmatism at the western Margin of the Ross Sea, Antarctica*.
- Muncy, H. L. (1979). *Geologic history and petrogenesis of alkaline volcanic rocks, Mount Morning, Antarctica. (MSc dissertation)*. http://rave.ohiolink.edu/etdc/view?acc_num=osu1124982704
- Naish, T., Powell, R., Levy, R., Wilson, G., Scherer, R., Talarico, F., et al. (2009). Obliquity-paced Pliocene West Antarctic ice sheet oscillations. *Nature*, 458, 322–328. <https://doi.org/10.1038/nature07867>
- Narcisi, B., Petit, J. R., Delmonte, B., Basile-Doelsch, I., & Maggi, V. (2005). Characteristics and sources of tephra layers in the EPICA-Dome C ice record (East Antarctica): Implications for past atmospheric circulation and ice core stratigraphic correlations. *Earth and Planetary Science Letters*, 239(3–4), 253–265. <https://doi.org/10.1016/j.epsl.2005.09.005>
- Narcisi, B., Petit, J. R., Delmonte, B., Scarchilli, C., & Stenni, B. (2012). A 16,000-yr tephra framework for the Antarctic ice sheet: A contribution from the new Talos Dome core. *Quaternary Science Reviews*, 49, 52–63. <https://doi.org/10.1016/j.quascirev.2012.06.011>
- Narcisi, B., Petit, J. R., & Langone, A. (2017). Last glacial tephra layers in the Talos Dome ice core (peripheral East Antarctic Plateau), with implications for chronostratigraphic correlations and regional volcanic history. *Quaternary Science Reviews*, 165, 111–126. <https://doi.org/10.1016/j.quascirev.2017.04.025>
- Nardini, I., Armienti, P., Rocchi, S., Dallai, L., & Harrison, D. (2009). Sr–Nd–Pb–He–O isotope and geochemical constraints on the genesis of Cenozoic magmas from the West Antarctic Rift. *Journal of Petrology*, 50, 1359–1375. <https://doi.org/10.1093/petrology/egn082>
- Niespolo, E. M., Rutte, D., Deino, A. L., & Renne, P. R. (2017). Intercalibration and age of the Alder Creek sanidine ⁴⁰Ar/³⁹Ar standard. *Quaternary Geochronology*, 39, 205–213. <https://doi.org/10.1016/j.quageo.2016.09.004>
- Noll, M. R. (1985). (p. 141). *Geochemistry and petrogenesis of the Alkaline lavas and their associated xenoliths, Mt. Overlord, Northern Victoria Land, Antarctica. (MSc Thesis) Retrieved from New Mexico Inst. of Mining and Technology*.
- Oppedal, L. T., van der Bilt, W. G. M., Balascio, N. L., & Bakke, J. (2018). Patagonian ash on sub-Antarctic South Georgia: Expanding the tephrostratigraphy of southern South America into the Atlantic sector of the Southern Ocean. *Journal of Quaternary Science*, 33, 482–486. <https://doi.org/10.1002/jqs.3035>
- Panther, K. S., Castillo, P., Krans, S., Deering, C., McIntosh, W., Valley, J. W., et al. (2018). Melt origin across a rifted continental margin: A case for subduction-related metasomatic agents in the lithospheric source of alkaline basalt, northwest Ross Sea, Antarctica. *Journal of Petrology*, 59, 517–558. <https://doi.org/10.1093/petrology/egy036>
- Panther, K. S., Hart, S. R., Kyle, P., Blusztajn, J., & Wilch, T. (2000). Geochemistry of Late Cenozoic basalts from the Cray Mountains: Characterization of mantle sources in Marie Byrd Land, Antarctica. *Chemical Geology*, 165(3–4), 215–241. [https://doi.org/10.1016/S0009-2541\(99\)00171-0](https://doi.org/10.1016/S0009-2541(99)00171-0)
- Panther, K. S., Kyle, P. R., & Smellie, J. L. (1997). Petrogenesis of a phonolite–trachyte succession at Mount Sidley, Marie Byrd Land, Antarctica. *Journal of Petrology*, 38(9), 1225–1253. <https://doi.org/10.1093/petroj/38.9.1225>
- Paulsen, T. S., & Wilson, T. J. (2010). Evolution of Neogene volcanism and stress patterns in the glaciated West Antarctic Rift, Marie Byrd Land, Antarctica. *Journal of the Geological Society*, 167, 401–416. <https://doi.org/10.1144/0016-76492009-044>
- Pearce, N. J. G., Perkins, W. T., Westgate, J. A., Gorton, M. P., Jackson, S. E., Neal, C. R., & Chenery, S. P. (1997). A compilation of new and published major and trace element data for NIST SRM 610 and NIST SRM 612 glass reference materials. *Geostandards Newsletter*, 21(1), 115–144. <https://doi.org/10.1111/j.1751-908X.1997.tb00538.x>
- Petrelli, M., Laeger, K., & Perugini, D. (2016a). High spatial resolution trace element determination of geological samples by laser ablation quadrupole plasma mass spectrometry: Implications for glass analysis in volcanic products. *Geosciences Journal*, 20, 851–863. <https://doi.org/10.1007/s12303-016-0007-z>
- Petrelli, M., Morgavi, D., Vetere, F., & Perugini, D. (2016b). Elemental imaging and petro-volcanological applications of an improved Laser Ablation Inductively Coupled Quadrupole Plasma Mass Spectrometry. *Periodico di Mineralogia*, 85(1). <https://doi.org/10.2451/2015PM0465>
- Petrelli, M., Perugini, D., Alagna, K. E., Poli, G., & Peccerillo, A. (2008). Spatially resolved and bulk trace element analysis by laser ablation - Inductively coupled plasma - Mass spectrometry (LA-ICP-MS). *Periodico di Mineralogia*, 77, 3–21. <https://doi.org/10.2451/2008PM0001>
- Phillips, E. H., Sims, K. W. W., Blichert-Toft, J., Aster, R. C., Gaetani, G. A., Kyle, P. R., et al. (2018). The nature and evolution of mantle upwelling at Ross Island, Antarctica, with implications for the source of HIMU lavas. *Earth and Planetary Science Letters*, 498, 38–53. <https://doi.org/10.1016/j.epsl.2018.05.049>
- Rasmussen, D. J., Kyle, P. R., Wallace, P. J., Sims, K. W., Gaetani, G. A., & Phillips, E. H. (2017). Understanding degassing and transport of CO₂-rich alkalic magmas at Ross Island, Antarctica using olivine-hosted melt inclusions. *Journal of Petrology*, 58(5), 841–861. <https://doi.org/10.1093/petrology/egx036>
- Rocchi, S., LeMasurier, W. E., & Di Vincenzo, G. (2006). Oligocene to Holocene erosion and glacial history in Marie Byrd Land, West Antarctica, inferred from exhumation of the Dorrel Rock intrusive complex and from volcano morphologies. *Bulletin Geological Society of America*, 118, 991–1005. <https://doi.org/10.1130/B25675.1>
- Rocchi, S., & Smellie, J. L. (2021). Chapter 5.1b Northern Victoria Land: Petrology. *Geological Society*, 55, 383–413. <https://doi.org/10.1144/M55-2019-19>
- Rocholl, A., Stein, M., Molzahn, M., Hart, S. R., & Wörner, G. (1995). Geochemical evolution of rift magmas by progressive tapping of a stratified mantle source beneath the Ross Sea Rift, Northern Victoria Land, Antarctica. *Earth and Planetary Science Letters*, 131(3–4), 207–224. [https://doi.org/10.1016/0012-821X\(95\)00024-7](https://doi.org/10.1016/0012-821X(95)00024-7)
- Scanlan, M. K. (2008). Petrology of inclusion-rich lavas at Minna Bluff, McMurdo Sound, Antarctica: Implications for magma origin, differentiation, and eruption dynamics. (MSc Thesis) Bowling Green State University. http://rave.ohiolink.edu/etdc/view?acc_num=bgsu1217952842
- Smellie, J. L. (1999). The upper Cenozoic tephra record in the south polar region: A review. *Global and Planetary Change*, 21(1–3), 51–70. [https://doi.org/10.1016/S0921-8181\(99\)00007-7](https://doi.org/10.1016/S0921-8181(99)00007-7)
- Stuckless, J. S., & Ericksen, R. L. (1976). Strontium isotopic geochemistry of the volcanic rocks and associated megacrysts and inclusions from Ross Island and vicinity, Antarctica. *Contributions to Mineralogy and Petrology*, 58(2), 111–126. <https://doi.org/10.1007/BF00382180>
- Sullivan, R. J. (2006). *The geology and geochemistry of seal crater, Hurricane ridge, Mount Morning, Antarctica*. <http://theses.otagogeology.org.nz/items/show/475>
- Tesi, T., Belt, S. T., Gariboldi, K., Muschitiello, F., Smik, L., Finocchiaro, F., et al. (2020). Resolving sea ice dynamics in the north-western Ross Sea during the last 2.6 ka: From seasonal to millennial timescales. *Quaternary Science Reviews*, 237, 106299. <https://doi.org/10.1016/j.quascirev.2020.106299>

- Timms, C. J. (2006). *Reconstruction of a grounded ice sheet in McMurdo Sound - evidence from southern Black Island*. <http://theses.otagoegology.org.nz/items/show/476>
- W. E. LeMasurier, & J. W. Thomson (Eds.), (1990). *Volcanoes of the Antarctic plate and southern oceans*. American Geophysical Union.
- Wartho, J.-A., Rex, D. D., & Guise, P. G. (1996). Excess argon in amphiboles linked to greenschist facies alteration in Kamila amphibolite belt, Kohistan island arc system, northern Pakistan: Insights from $^{40}\text{Ar}/^{39}\text{Ar}$ step-heating and acid leaching experiments. *Geological Magazine*, *133*(5), 595–609. <https://doi.org/10.1017/s0016756800007871>
- Wilch, T. I., McIntosh, W. C., & Dunbar, N. W. (1999). Late Quaternary volcanic activity in Marie Byrd Land: Potential $^{40}\text{Ar}/^{39}\text{Ar}$ -dated time horizons in West Antarctic ice and marine cores. *Geological Society of America Bulletin*, *111*, 1563–1580. [https://doi.org/10.1130/0016-7606\(1999\)111<1563:LQVAIM>2.3.CO;2](https://doi.org/10.1130/0016-7606(1999)111<1563:LQVAIM>2.3.CO;2)
- Worner, G., Viereck, L., Hertogen, J., & Niephaus, H. (1989). The Mt. Melbourne Volcanic Field (Victoria Land, Antarctica) II: Geochemistry and magmagenesis. *Geologisches Jahrbuch*, *E38*, 395–433.
- Wright-Grassham, A. C. (1987). *Volcanic geology, mineralogy, and petrogenesis of the discovery volcanic subprovince, southern Victoria land, Antarctica*. (PhD dissertation) (p. 460). New Mexico Institute of Mining and Technology.
- Yan, Y., Bender, M. L., Brook, E. J., Clifford, H. M., Kemeny, P. C., Kurbatov, A. V., et al. (2019). Two-million-year-old snapshots of atmospheric gases from Antarctic ice. *Nature*, *574*(7780), 663–666. <https://doi.org/10.1038/s41586-019-1692-3>